GEOPHYSICAL STUDIES RELATED TO THE PROPOSED LOW-LEVEL RADIOACTIVE
WASTE REPOSITORY, HUDSPETH COUNTY, TEXAS

by

G. R. Keller, Diane I. Doser, and Mark Baker

Final Contract Report

Prepared for

Texas Low-Level Radioactive Waste Disposal Authority
under Interagency Contract Number IAC(90-91)0268

by

Bureau of Economic Geology
W. L. Fisher, Director
The University of Texas at Austin
Austin, Texas 78713

June 1990

CONTENTS

SEISMIC REFLECTION SURVEY FOR THE PROPOSED LOW-LEVEL RADIOACTIVE WASTE REPOSITORY, HUDSPETH COUNTY, TEXAS

Mark Baker and G. R. Keller

Department of Geological Sciences

The University of Texas at El Paso

INTRODUCTION

Geologic characterization of sites for low-level radioactive waste repositories generally requires qualitative and quantitative estimates of variations in rock properties between test wells. Seismic reflection surveys are an accepted technique for providing a qualitative picture of structural and/or stratigraphic variation when tied closely to control information from wells. Reflection surveys also are useful in identifying areas where additional well control may be needed to adequately characterize geologic variations.

Ten miles (16 km) of reconnaissance seismic data was collected and interpreted by Phillips et al. (1986) in the vicinity of the proposed repository site near Fort Hancock, Hudspeth County, Texas. Three lines were collected perpendicular to the major structural trends, and a fourth line tied these three together. These data typically resolve variations in stratigraphic thickness that are more than 20 ft (6 m) thick, 1/4 the dominant time wavelength, and that are more than 90 ft (27 m) deep. These data can image horizontal variations greater than 110 ft (34 m), 8 common depth point samples per wavenumber.

Phillips et al. (1986) interpreted these lines and constructed isochron maps on the top of the Cretaceous bedrock, the top of the basal Older Bolson deposits, and the base of the Younger Bolson deposits. Two major faults cutting Cretaceous through Younger Bolson deposits were interpreted near the study area. These interpreted faults parallel the structural trend of the Campo

1

Grande fault. Phillips et al. (1986) reported severe problems in data collection associated with air-blast from the vibrator. Additional difficulties degrading data quality in this survey, visible on their trace displays, include surface statics, significant dispersive surface wave energy, spatial aliasing, and attenuation of high-frequency arrivals. Many of these problems in collecting high-quality data are directly related to the near-surface geology. The discontinuous, variable-thickness, high-velocity caliche layer near the surface gives a strong air-blast, dispersive surface wave, static problems, and a high proportion of shot energy coupled into nonlinear, near-field waves. The nature of alluvial deposition in the area gives rise to significant deviations from two-dimensional layering, with consequent out-of-plane reflections, apparent static problems, and spatial aliasing. The near-surface unconsolidated gravels and deep water table result in high scattering and attenuation of high-frequency waves.

The purpose of this study was twofold. First, we needed to determine whether data could be collected with resolution adequate to characterize the geology, within a finite budget. Second, we wanted to better describe the extent of faulting and stratigraphic variation in the vicinity of the proposed low-level radioactive waste repository site. Our first step was to perform noise tests to find recording parameters that might give resolution adequate for the second stage of data collection. We chose to use a land air gun with a small chamber as source, as previous experience indicated that it could generate adequate high frequencies with these near-surface conditions. The air gun is less expensive than the preferred small explosive charges in shallow holes. We also chose to use higher frequency 40 Hz phones to emphasize high frequencies.

Following initial tests to determine optimum recording parameters, a short section of line was recorded and processed. This line demonstrated that resolution could be improved over the data collected by Phillips et al. (1986), and the remainder of the planned seismic survey was collected.

SEISMIC LINE LOCATIONS

Three seismic lines were collected in this study (Table 1). The first line (UTEP-1) duplicates portions of lines UT-3B and UT-3A described by Phillips et al. (1986), and the other two lines (UTEP-2, UTEP-3) cover previously unsurveyed terrain. Figure 1 shows the locations of the three seismic lines superimposed on the map of seismic lines run in the previous survey (Phillips et al., 1986). Table 1 gives locations of the endpoints of the lines digitized from maps, associated shot-point numbers, and an estimate of the line location relative to the previous survey. The three lines are located relative to cultural features on 7.5-minute topographic maps where available and are surveyed relative to line UTEP-1 where culture is not reliable. Relative elevations of each shot point were surveyed for static corrections with an overall accuracy of less than 0.2 ft (6 cm).

Line UTEP-1, located along the main access road, duplicated previous seismic survey coverage for four reasons. First, higher resolution seismic information was required in the vicinity of the study area, and the road crossed several faults interpreted in the previous seismic survey. Second, an initial feasibility survey was required to determine if data of adequate resolution could be collected despite the poor near-surface conditions in the area; the first section of line UTEP-1 provides a direct comparison with a poor-data area from the previous survey (Phillips et al., 1986; this study, Figure 4). Third, the access road provided optimum source-receiver coupling conditions in that the road has been graded down to the competent caliche layer. Finally, considerable vehicular traffic is required in the first noise tests, and we wished to minimize off-road damage. Shot-point numbering on line UTEP-1 differs from that on the other lines because the original staking and surveying of the line used actual footage from the line start prior to establishing the shot-point spacing.

Line UTEP-2 runs nearly east-west, and is intended primarily to be a tie between UTEP-1 and UTEP-3. This line is near the southern limit of the repository study area.

Line UTEP-3 parallels line UTEP-1 and follows a preexisting bulldozer track that passes a well. This line provides additional control on the orientation of a structure that might be interpreted on line UTEP-1.

Elevations of geophones and shot points were measured on all three lines relative to shot point 0 on line UTEP-1 using a Wild LS3B auto-level. Each time the level was repositioned three duplicate shot-point elevations were measured. Absolute maximum closure errors for the three lines are as follows: UTEP-1, 0.18 inch (0.46 cm), UTEP-2, 0.07 inch (0.18 cm), and UTEP-3, 0.09 inch (0.23 cm). Plots of the relative elevations of the three lines are shown in Figure 2.

DATA ACQUISITION

Data acquisition encompassed two major phases. The first phase involved testing of source and receiver configurations on a noise walkaway test in which a short segment of seismic line with the preferred configurations to test data quality. After the tests and short section of line were processed and displayed, the second phase of data collection along the three lines was begun.

FIRST-PHASE DATA ACQUISITION

Two noise walkaway tests were performed using different source and receiver configurations (Table 2). The first consisted of single geophones on a 5-ft (1.5-m) spacing with the source stepped out 140 ft (42.7 m) on each shot up to a distance of 1,320 ft (402.4 m). Up to 30 shots per station were recorded. The second test consisted of groups of nine geophones, in weighted and unweighted arrays, with a 15-ft (4.6-m) spacing. All geophones were planted with spikes in the caliche in the roadbed along line UTEP-1 and buried.

The following conclusions were reached from field records and initial playbacks:

4

(1) Multiple shots at a given shot point gave little effective improvement in signal-to-noise ratio (S/N). Figure 3a from one shot shows little noise reduction in comparison with Figure 3b from 20 shots. One shot per shot point was used in subsequent data collection.

(2) Geophone spreads more than 30 ft (9 m) long would be required to begin to effectively reduce noise from the air and surface waves. The near-surface resolution required to answer the geologic questions posed is impossible with the extensive spatial averaging of such arrays. Single phones were used in subsequent tests.

(3) Significant lateral near-surface discontinuities form a second significant source of shot-associated noise, as is evident in Figure 4c. Lateral discontinuity of deeper reflectors at longer offsets seen in Figure 4a indicates that a geophone spacing of more than 10 ft (3 m) would reduce the quality of normal moveout corrections. A 15-ft (4.6-m) geophone spacing was a compromise to permit completion of the survey within budget.

(4) The strong lateral near-surface discontinuities and the dominant shot-associated noise visible on Figures 4c and 4b indicate that long offsets and high fold are required to image the near-surface velocity variations. A recording geometry was chosen in which 56 channels with 15-ft (4.6-m) spacing were shot off both ends, giving an effective split spread configuration with 56 fold.

Following the noise walkaway tests a 1,300-ft (396-m) section of line UTEP-1 was recorded. The location of this test line corresponds to the section of line UT-3b between shot points 560 and 520. Figures 5a and 5b compare a rough stack from this survey with the final processed result from UT-3b. The rough stack of Figure 5a has not been deconvolved, resulting in a distinct ringing, and has not been velocity filtered to remove shot-associated noise. Even so, coherency and resolution of reflections have been improved by using the closer spacing and higher fold of this study. Imaging of near-surface reflections has also been improved over that of line UT-3b in that coherent energy is visible up to 60 ms. on Figure 5a, compared to 140 ms. on Figure 5b. The improved coherency from 60 to 140 ms. and from 200 to 300 ms. on Figure 5a led us to

5

conclude that shot-associated noise and spatial aliasing were the probable cause of the poor-data areas on line UT-3b, and that the improved data quality warranted continued data collection.

While results from this test line were being processed, additional tests were run on changing the source strength. These unusual tests were performed because the previous experience of the contractor and first author indicated that source strength has a strong control on S/N on near-surface reflections. Air-gun pressures were varied from 1,100 to 1,750 psi and field records compared. Two conclusions were reached from these tests. First, lowering the gun pressure reduced the frequency content of close reflections. Second, the first 500 ms. of several near traces were thoroughly overwhelmed by incoherent shot noise nonlinearly related to shot amplitude at all gun pressures. Consequently, we chose to shoot the gun at 1,750 psi to maximize high frequency content, and we introduced an offset from the shot to the first receiver of three shot points of 45 ft (13.5 m).

SECOND-PHASE DATA ACQUISITION

After review of the test section, data collection continued on the three lines. Relevant information on acquisition parameters is summarized in Table 2. In addition to the reflection recording parameters, reversed refraction profiles with offsets up to 2,500 ft (760 m) were routinely recorded along the line.

One significant change was made between lines by changing from 60 Hz low-cut filters on line UTEP-1 to 27 Hz low-cut filters on lines UTEP-2 and UTEP-3. This change was made as line UTEP-1 was recorded along the main road with both shots and receivers well coupled to the caliche. Lines UTEP-2 and UTEP-3 ran cross country, with source and geophones coupling through poorly consolidated alluvium.

When this line was initially proposed, we expected to use a high-frequency baseplate on the air gun in areas where the near-surface materials were unconsolidated. When tested here, the high-frequency baseplate increased shot-associated noise and was not used in routine data collection.

6

GEOLOGIC SETTING

Stratigraphic nomenclature and geologic descriptions of strata in the vicinity of this study are primarily from Collins and Raney (1989), who provide more complete references to previous geologic studies. This nomenclature is summarized in Table 3. Aspects of this description of the geologic setting not taken from Collins and Raney will be specifically quoted.

The seismic lines are located within a small foreland basin of Tertiary age bounded on the southwest by Cretaceous strata thrust toward the northeast, and on the north by the Diablo Plateau. Subsequent extensional faulting, beginning about 24 Ma ago, resulted in formation of the Hueco Bolson with the Campo Grande fault trend comprising one of the northeast boundary faults (Figure 1). The northeastern edge of the thrust sheet has been interpreted to lie approximately 2 to 3 mi (4 to 5 km) northeast of the trace of the Campo Grande fault and about 0.6 mi (1 km) northeast of the start of seismic line UTEP-1.

Cretaceous strata crop out in the Diablo Plateau, dipping 5 to 8 degrees to the southwest near the rim fault. These strata also crop out at Campo Grande Mountain and form a syncline and overturned anticline with strata dipping to the southwest. From previous seismic surveys, Cretaceous strata between the north side of the study area and the thrust margin have been interpreted to dip southwestward at a low angle. A rough estimate from seismic line UT-3A (Phillips et al., 1986) indicates a dip of 7 degrees.

The Tertiary Fort Hancock Formation unconformably overlies Cretaceous strata in the study area. Where the Fort Hancock Formation crops out in the region, it is composed of clay, silt, and sand. However, the Fort Hancock Formation may locally contain conglomeratic strata from debris shed off the nearby topographic highs of the thrust sheet, although this is rarely seen in outcrop. The water table is mostly located within the Fort Hancock Formation, and the associated velocity increase will probably give a significant reflection compared to internal stratification.

The Camp Rice Formation unconformably overlies the Fort Hancock Formation. These sediments are composed of sand and gravel and represent alluvial fan, fluvial, and minor lacustrine and floodplain deposits. Erosion of the underlying Fort Hancock strata, visible in Alamo Arroyo (Collins and Raney, 1989), is consistent with a regional change in the equilibrium topographic profile from formation of the Hueco Basin. The truncation surface should be apparent on the seismic profiles if resolution of near-surface reflectors is adequate.

Regional Pleistocene deposits include the Madden through Balluco Gravels. These gravel deposits are thin and have local caliche; they affect the seismic section interpretation only through addition of noise and scattering.

SEISMIC INTERPRETATION

The seismic data are interpreted by first establishing the relationship between reflections and the stratigraphy, and then by relating the reflection patterns to structural causes. This approach is taken because there is ambiguity in attributing reflections to structure or stratigraphy alone, and stratigraphic variations across the study area are evident from the seismic data of Phillips et al. (1986).

The stratigraphic portion of this section will describe criteria for recognizing Cretaceous strata and the Fort Hancock Formation and will indicate why the Camp Rice Formation is not recognizable. The structural portion of this section will (1) discuss a reinterpretation of the two faults interpreted by Phillips et al. (1986) and then (2) describe the association with fissuring observed in the area.

CRETACEOUS STRATA

Cretaceous stratigraphy is most readily identifiable through consistent thickness, uniform reflections that dip to the southwest, visible below 350 milliseconds (ms) in Figures 6 through 9

(in pocket). In most cases the top of the Cretaceous strata can be identified by erosional truncation of these reflections. This truncation is most evident in Figures 6 and 7; it is more readily visible in Figure 6 as it is scaled to give about 1.3:1 vertical exaggeration whereas Figure 7 has about a 1.6:1 horizontal exaggeration in the Cretaceous.

There is one distinctive stratigraphic unit within the Cretaceous most readily visible between 350 and 400 ms (250 ft thick) from CDP 680-740 (Figure 6a). This unit has consistent reflections from internal cross-stratification with horizontal dimensions of 100 ft (30.5 m) and vertical dimensions of about 30 ft (9.1 m, 7 ms). This unit occurs consistently across the study area and is useful to constrain structural deformation within the Cretaceous strata. The depth and thickness of this unit are consistent with a tentative identification as the Cox Sandstone, but this is speculative without well control.

The reinterpreted top of the Cretaceous strata is shown in both Figures 6 and 7. The lowest point of the Cretaceous top occurs from SP 560 to 700 in Figure 6. This is recognizable by the contrast between relatively flatlying Cretaceous reflectors and downlapping alluvium apparently shed off the topographic high between SP 740 and SP 790. The 310 ms relief between the topographic high and the deep basin is consistent with the Bouguer gravity anomaly of 2.8 mgals, a density contrast of 0.35 gm/cc, and an average velocity of the interval of 4,000 ft per second (ft/sec). This places the deepest part of the basin about 620 ft (189 m) below the topographic high, or about 820 ft (250 m) below the surface (Keller, this report).

A tie point with well data occurs near CDP 110 (Figure 7) where wells 72 and 73 penetrate to the Cretaceous near the seismic line (Gustavson, 1990). The Cretaceous top is found at 720 ft (220 m) depth, consistent with a 370 ms arrival time and an average velocity from the surface of 4,000 ft/sec.

The top of Cretaceous strata is additionally identified by the tendency of reflectors to correlate with topography of the Cretaceous surface (velocity pullup). Since the Cretaceous strata are of significantly higher velocity than the Fort Hancock Formation strata, an increase in thickness in the Fort Hancock Formation will lead to an increase in two-way travel time. Velocity pullup is seen

9

below topographic highs at CDP 1340, CDP 790, and CDP 700 in Figure 7. This pullup is also visible throughout Figure 6 beneath changes in elevation of the Cretaceous topography.

FORT HANCOCK FORMATION

Primary seismic attributes for recognizing deposits in the Fort Hancock Formation are clinoform reflections from fluvial channels. The lower interval velocities of about 4,000 ft/sec to 7000 ft/sec in the Fort Hancock Formation give the seismic section of Figure 7 about a 1:1 vertical exaggeration, in contrast to the 2.2:1 vertical exaggeration of Figure 6. There is some difficulty in distinguishing these fluvial strata where dip is similar to the Cretaceous surfaces, such as near CDP 810 and well 72 (Figure 7). Differentiation relies on velocity pullup in the Cretaceous strata.

Strata above the Cretaceous in well 73 include two 50- to 70-ft-thick fluvial sand bodies separated by clay beds, overlying a basal conglomerate (Gustavson, 1990). These strata are consistent with the three well-defined reflectors between 290 ms and 330 ms from CDP 40 to CDP 240 on Figure 7.

The top of these well-bedded reflectors associated with fluvial strata in well 73 coincides with the elevation of the water table (preliminary BEG water table map) and with the top of the basal Older Bolson Deposit of Phillips et al. (1986) on Figure 6. This horizon is visible as a strong reflector on Figure 6 and appears to be an erosional surface on the higher resolution data in Figure 7. This surface separates southwest-dipping fluvial deposits, that appear truncated on top, from overlying flatlying deposits with slightly downlapping reflectors toward the northeast. This apparent erosional truncation might be associated with lowering of depositional base level during subsidence of the main portion of the Hueco Bolson.

Reflectors above the fluvial Fort Hancock deposits (150 ms to 250 ms) are interpreted to represent very well bedded strata of uniform thickness that are locally broken by apparent channels. These units are consistent with deposits in a restricted basin that range from lacustrine to intermittent stream deposits. Between 100 ms and 150 ms the reflectors appear to be more regular

10

with braided stream deposits in places, but data quality is starting to deteriorate from near-surface noise. These reflectors above the water table have velocities from 2,000 ft/sec to 4,000 ft/sec with apparent vertical exaggerations of 4.4:1 (Figure 6) and 2:1 (Figures 7 through 9).

CAMP RICE FORMATION

The contact of the Camp Rice Formation with the Fort Hancock Formation is not visible on any of the sections collected to date. Shear velocities estimated from surface-wave measurements (Nazarian, 1990) indicate a relatively high velocity zone from about 20 ft (6.1 m) to 40 ft (12.2 m) in depth in many places. Conversion of these shear velocities to compressional velocities (assuming a conservative Vp/Vs ratio of 1.4 for unconsolidated, unsaturated sediment) would place the top of the Fort Hancock Formation at a 70 ms two-way travel time.

Initial processing results from data collected in this survey indicated that we might be able to image the Camp Rice reflectors, but subsequent processing showed that we were probably stacking refracted arrivals from discontinuous high-velocity layers in the near surface. The strength of this "noise" was apparent in the noise walkaway tests, and it was not possible to remove it by further processing.

Structural Interpretation

The seismic reflection survey of Phillips et al. (1986) recognized two areas with significant reflector discontinuity which they interpreted as possibly being due to normal faulting. The seismic data collected in this survey more clearly image these two anomalous areas, and the subsequent discussion will deal with the southwest area first and then the northeast area.

The southwest area of interest (Figure 6b) is located between SP 411 and SP 466, corresponding to CDP 445 and CDP 660 in Figure 7a. The fault was originally interpreted on the basis of continuous but offset reflections at 270 ms, discontinuous, offset reflections within the

11

Cretaceous strata down to 500 ms, and thickening of the Fort Hancock Formation by 20 ms southwest of the fault (Figure 6b).

Thickening of the Fort Hancock Formation and some discontinuous reflections that form the basis of the interpreted fault in Figure 6 are present on the higher resolution seismic section of Figure 7. The minor disruption of reflections in the Cretaceous section is more readily attributable to velocity pullup beneath the higher Cretaceous topography at CDP 570. Reflector disruption is consistently under the southwest-dipping Cretaceous surface between CDP 540 and CDP 580 and would imply a near vertical fault if it were not so closely associated with the topography. Projection of the fault onto line UTEP-1 and extension of the trend onto line UTEP-2 (Figure 8) show little basis for recognition of structural deformation.

Offset on the interpreted basal Older Bolson Deposit noted by Phillips et al. (1986) is seen in Figure 7 to be a clinoform truncated by an erosional surface. Differential compaction of Fort Hancock sediments over the Cretaceous bedrock surface, along with out-of-plane reflections from the Cretaceous topography in this area can account for most of the reflector disruption within the lower Fort Hancock Formation between CDP 280 and CDP 520. Reflector disruption within the upper Fort Hancock Formation appears to be more closely associated with depositional features. If any of these disruptions are associated with faulting, the faulting cannot be traced into the Cretaceous bedrock.

The origin of the Cretaceous topography in the southwest area is puzzling. Extrapolation of the trend of the thrust fault encountered in the Krupp No. 1 Thaxton well (Collins and Raney, 1989) should bring it to the Cretaceous surface in this area. There is strong evidence of folding (CDP 160-260) and thickening (CDP 400-480) in the Cretaceous units, but there are no indications of a thrust cutting across bedding in the section. A bedding plane thrust could be interpreted in several areas.

The northeast area of interest (Figure 6b) is located between SP 251 and SP 268, corresponding to CDP 1230 and CDP 1170 in Figure 7. The normal fault interpreted by Phillips et al. (1986) does not have clearly defined reflector discontinuities, but Phillips inferred that the

Cretaceous and lower Fort Hancock strata are structurally lower to the southwest, with associated thickening of the upper Fort Hancock Formation.

Interpretation of the higher resolution seismic data in Figure 7 shows complex structure in the Cretaceous strata. The major feature is a southwest-thinning wedge of truncated Cretaceous reflectors between 310 ms and 410 ms from CDP 1060 to CDP 1280. Upper reflectors of the wedge are truncated, and the lower reflectors dip to the northeast in opposition to Cretaceous topography. The cross-stratified Cretaceous unit interpreted as the Cox Sandstone thickens between CDP 980 and CDP 1140 and appears to climb over the wedge. This wedge is interpreted as a thrust ramp, the overlying cross-stratified unit being thickened by back thrusting. Seismic line UTEP-3 (Figure 9) appears to begin to encounter this wedge at about CDP 620, but unfortunately it is poorly resolved at the edge of the data set.

Several small normal faults could be interpreted from reflection disruption within the lower Fort Hancock and the Cretaceous above the thrust fault. These faults do not cut the thrust plane and might be associated with isostatic response to thrust loading. There also appears to be no correlatable offset of reflectors above the fluvial Fort Hancock strata. These disruptions of reflectors in the fluvial Fort Hancock could also be associated with limits of fluvial deposition controlled by the Cretaceous topography.

The trend of the surface fissures found in this area intersect the seismic line at about CDP 1160 (Figure 7). The horizontal attitude of Cretaceous strata at 400 ms around this point indicates that flexure may have taken place in response to thrust loading. There is also a change in surface topography at this point with Figure 2 showing a concave upward profile to the northeast, and a concave downward profile to the southwest. Modeling of gravity data by Keller (1990) has shown that the Cretaceous section also reaches its maximum thickness here. There is no evidence that through-going, high-angle faults are present in Tertiary or younger strata in this area.

The occurrence of breaks in slope apparent on line UTEP-1 in the survey data of Figure 2 have been plotted on Figure 7 using the characters SC. These do not appear to correlate with reflector disruptions interpretable as faults within the Fort Hancock Formation.

CONCLUSIONS

Interpretation of seismic data collected in this survey indicates that potential normal faults interpreted by Phillips et al. (1986) do not significantly offset Cretaceous strata and probably do not have measurable offset in the Fort Hancock Formation that can be readily resolved in the seismic sections. Many of the disrupted reflectors visible in the early survey appear to be sedimentologic features associate with fluvial deposition in the early stages of basin filling. A zone of structural complexity in the Cretaceous, near the northeastern fault interpreted by Phillips et al. (1986), has been interpreted as a thrust ramp. This zone of structural complexity appears to have flexed after loading and may be associated with small-scale normal faulting in early Pliocene deposits. It also underlies the area of fissures that occur in surficial deposits.

REFERENCES

Collins, E. W., and Raney, J. A., 1989, Description and Quaternary history of the Campo Grande Fault of the Hueco Basin, Hudspeth and El Paso Counties, Trans-Pecos Texas: The University of Texas at Austin, Bureau of Economic Geology, contract report prepared for the Texas Low-Level Radioactive Waste Disposal Authority, 61 p.

Gustavson, T. C., 1990, Stratigraphic cross section, Tertiary to Quaternary strata, Texas low-level radioactive waste disposal study area, Hueco Bolson, West Texas: The University of Texas at Austin, Bureau of Economic Geology, draft contract report.

Phillips, J. D., Dean, D. F., and Riherd, P. S., 1986, Preliminary seismic reflection study of the Fort Hancock area in Hudspeth County, Texas: The University of Texas at Austin, Institute for Geophysics, contract report.
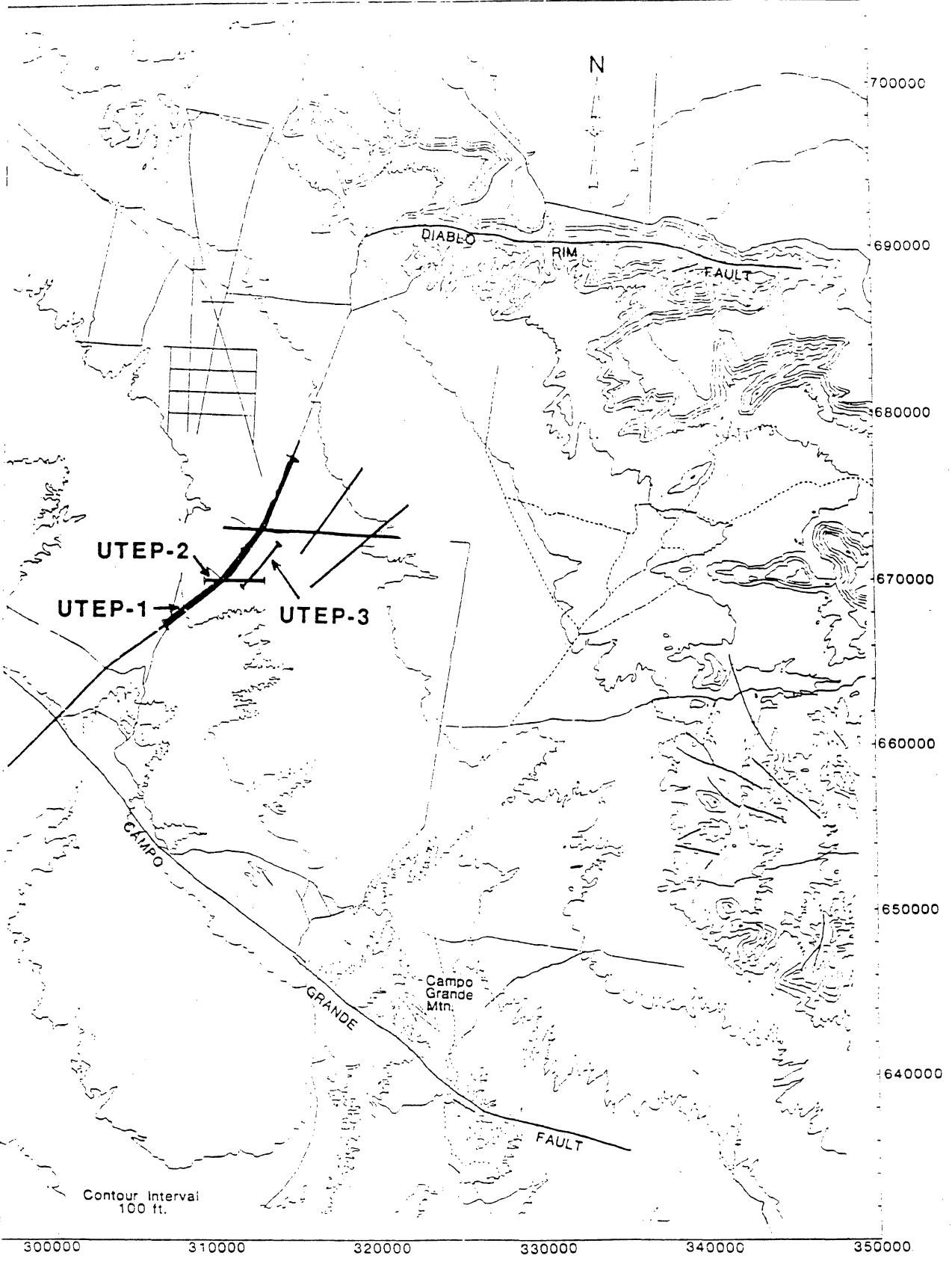
Figure 1. Regional base map showing locations of seismic lines collected in this survey (UTEP-1, UTEP-2, UTEP-3), and those lines collected in a previous survey by Phillips and others (1986).
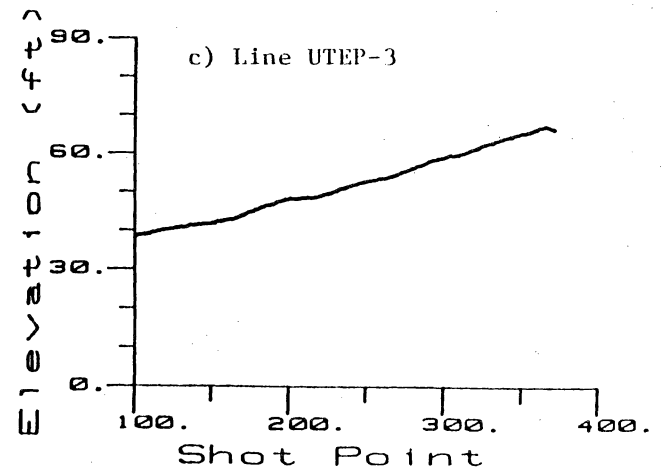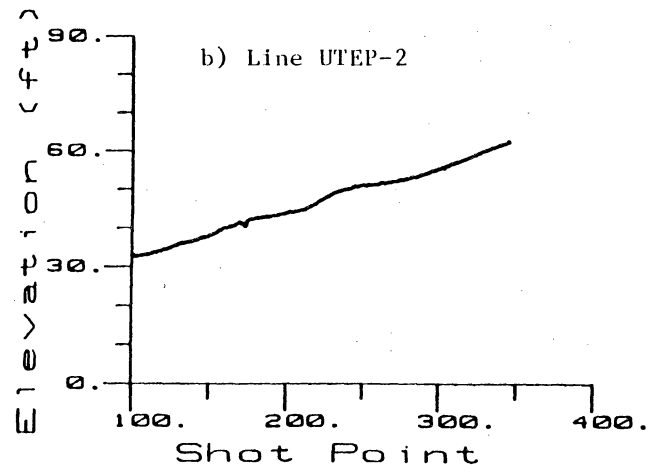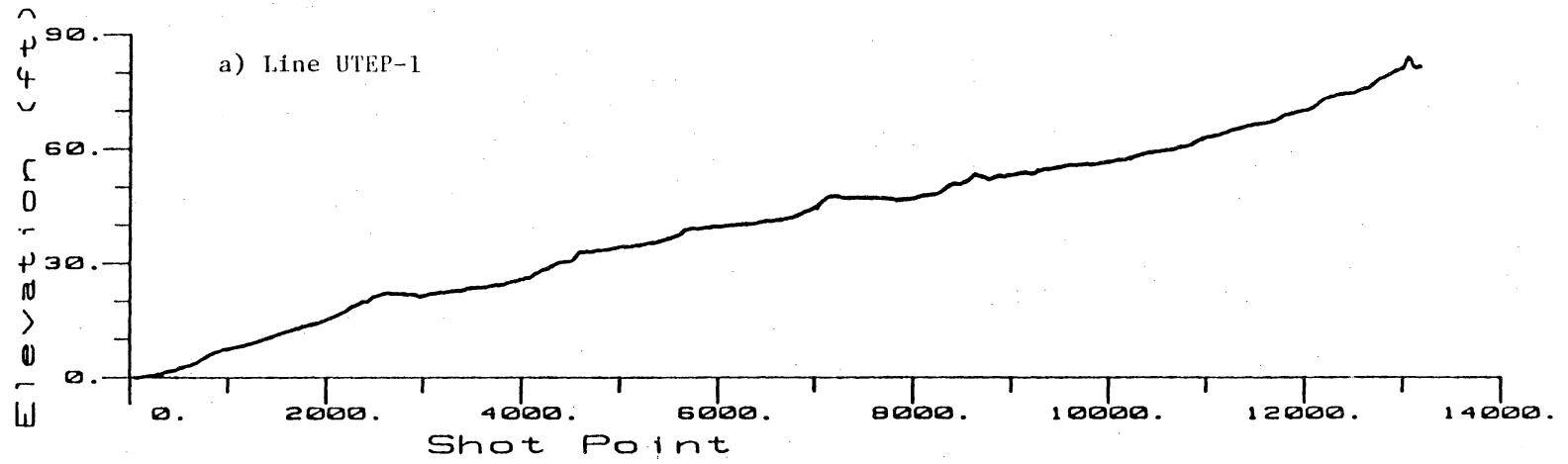
Figure 2. Elevation plots for the seismic lines relative to shot point 0, line UTEP-1.
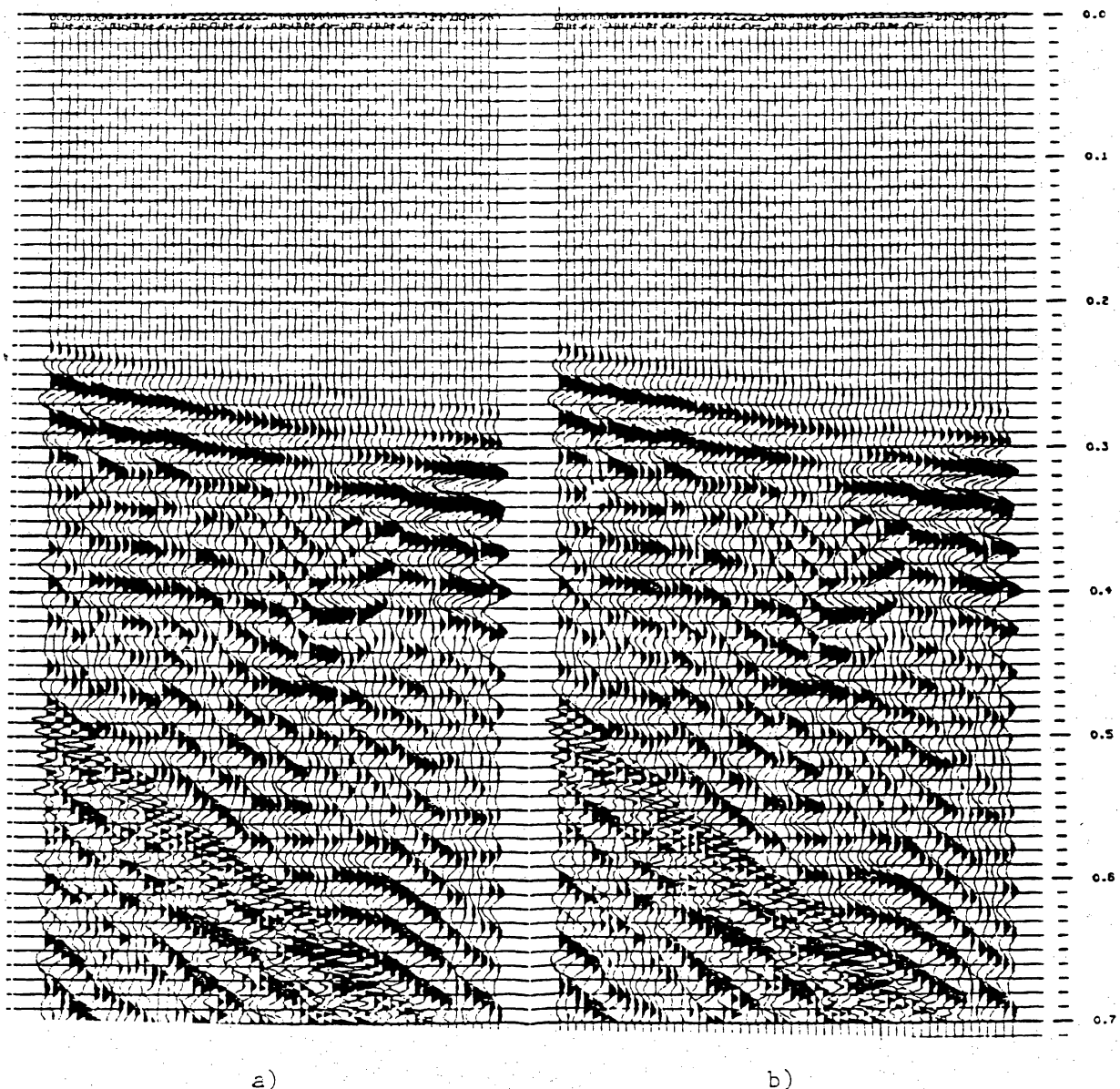
Figure 3. (a) Common shot gather for one shot compared with (b) a common shot gather for 20 stacked shots.
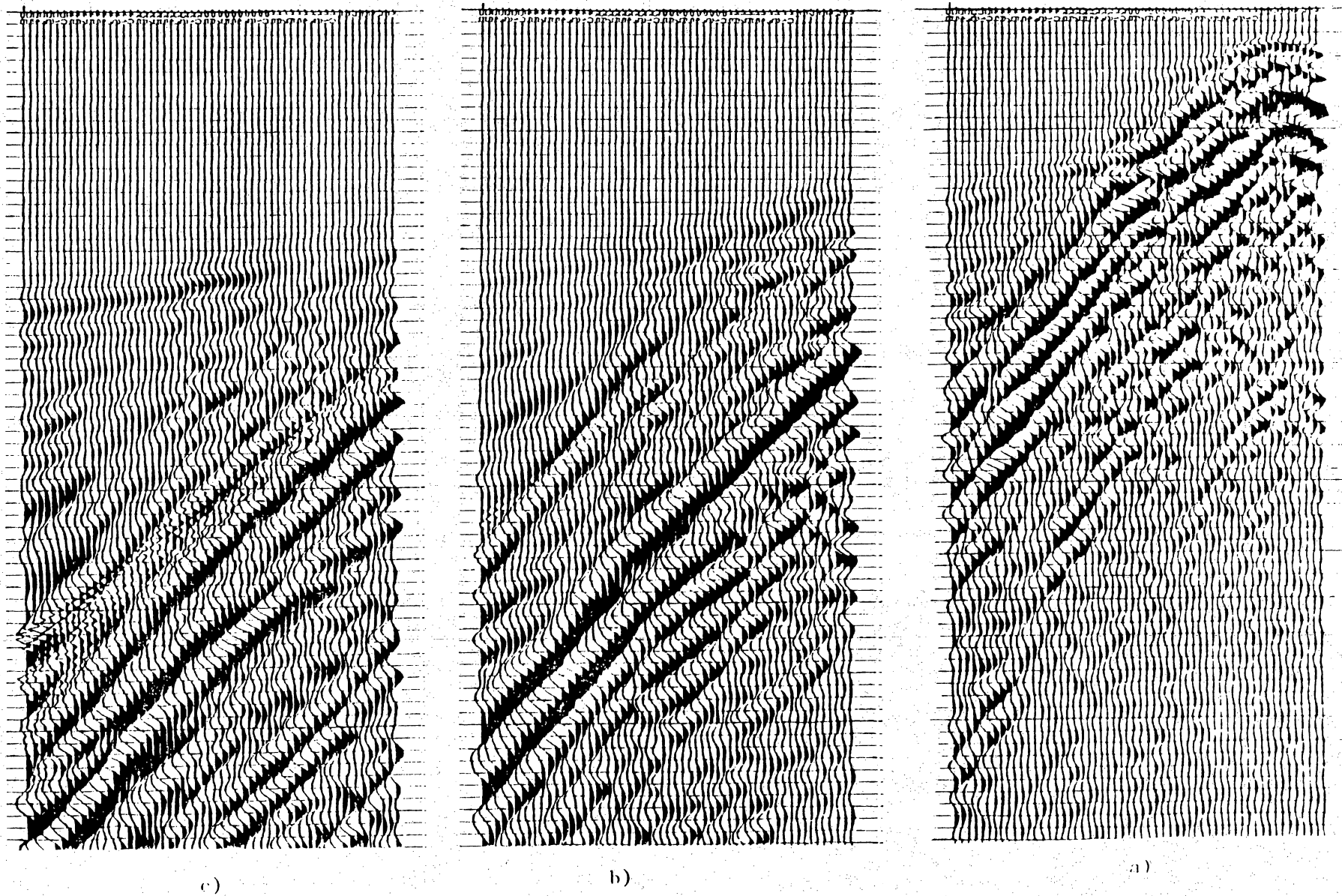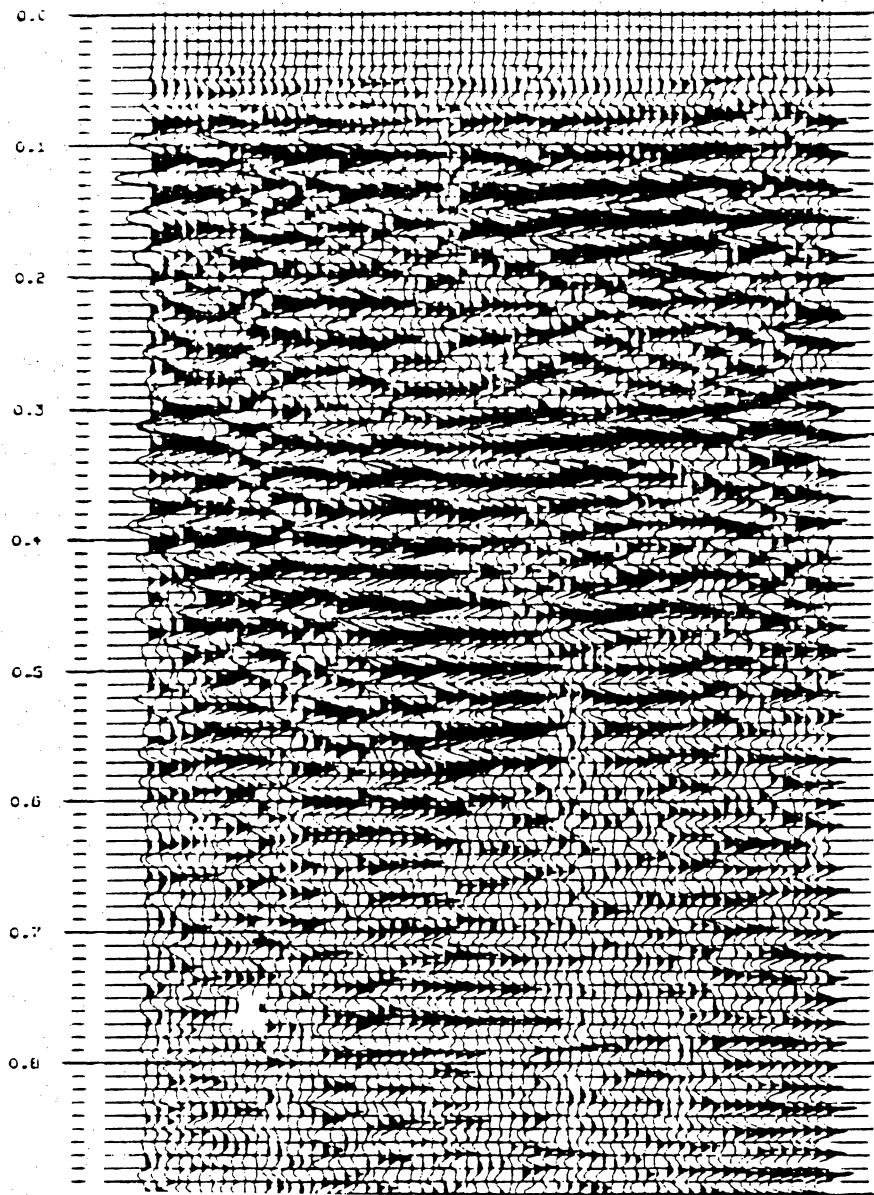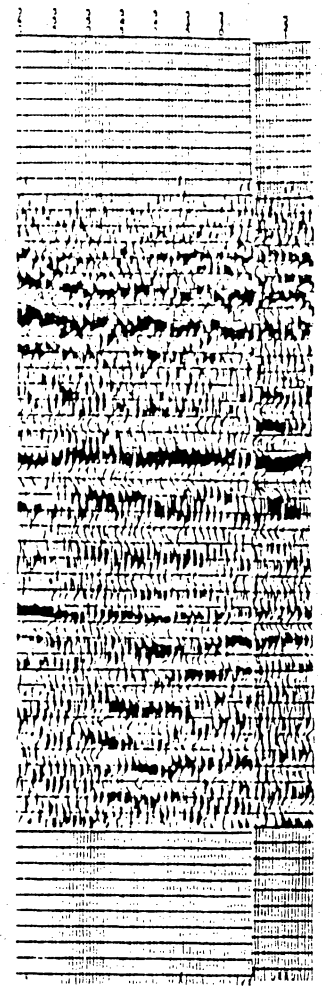
18

Figure 4. Common shot gathers from the noise walkaway test with receivers on a 5-ft spacing.
(a) Shot in receiver spread. (b) Shot 330 ft from first trace. (c) Shot 570 ft from first trace.

Figure 5 (a). Brute stack from initial test line along UTEP-1 compared with (b) section of line UT-3B corresponding to same area.

Table 1. Seismic line locations.

Line	Line Start	Line End
UTEP-1	31° 23' 6.24" –105° 45' 40.20" Shot point 0 UT-3B Shot point 561	31° 25' 1.62" –105° 44' 12.12" Shot point 13200 UT-3A Shot point 81
UTEP-2	31° 23' 29.28" –105° 45' 11.04" Shot point 100	31° 23' 28.20" –105° 44' 27.90" Shot point 346
UTEP-3	31° 23' 23.82" –105° 44' 43.20" Shot point 100	31° 23' 48.06" –105° 44' 13.50" Shot point 270

Table 2. Seismic survey field acquisition parameters.

Seismic Contractor	Cam Walker Walker Geophysical 311 East Street Essex, Iowa 51638 (712) 379-3499
Processing Contractor	Clyde Lee Sytec 3939 Ann Arbor Houstin, Texas 77063 (713) 783-9540
Source	Bolt LSS-3B Land Air Gun, 20 c.i. chamber, 1750 psi.
Shot Point Spacing	15 ft
Shots per Shot Point	1
Geophone Spacing	15 ft
Geophones	Mark Products, 40 Hz, L25E 66% damping Single phone per location
Recording Geometry	Split spread 885'-45' – 45'-885'
Recording Instrument	DFS-V 56 channels 1 ms sample rate 1.25 s. records
Filters	250 Hz anti-alias high-cut 60 Hz, 18dB/oct low-cut (UTEP-1) 27 Hz, 36dB/oct low-cut (UTEP-2,3)

Table 3. Stratigraphic Column

Age	Stage	Name: thickness		
Quaternary	Holocene	Qt	Terrace Alluvium	
Quaternary	Pleistocene	Qb	Balluco Gravel	(8 ft)
Quaternary	Pleistocene	Qr	Ramey Gravel	(8 ft)
Quaternary	Pleistocene	Qm	Madden Gravel	
Tertiary	Pliocene	QTcr	Camp Rice Fm. (50 ft thick)	
Tertiary	Pliocene	Tfh	Fort Hancock Fm. (800 ft thick)	
Cretaceous	Comanchean	Kf	Finlay Ls.	
Cretaceous	Comanchean	Kc	Cox Ss.	
Cretaceous	Comanchean	Kb	Bluff Mesa	

SEISMOLOGICAL STUDIES FOR THE PROPOSED LOW-LEVEL RADIOACTIVE WASTE REPOSITORY, HUDSPETH COUNTY, TEXAS

Diane I. Doser

Kidd Seismological Observatory

Department of Geological Sciences

The University of Texas at El Paso

INTRODUCTION

The proposed site of the Texas low-level radioactive waste repository in Hudspeth County is within the Hueco Basin of Trans-Pecos Texas (Figure 1). The Hueco Basin, or Hueco Bolson, contains several fault systems of Quaternary age and has been the site of several felt earthquakes. A study of the recent tectonic history and seismicity of the Hueco Bolson and surrounding regions is important for assessing potential earthquake hazards at the study area and for designing a seismically safe repository.

The first section of this report will briefly discuss the tectonic history of the Hueco Bolson and its relation to the development of the southern Basin and Range and the Rio Grande rift. Stress measurements that indicate that the region is still undergoing extension, predominantly along normal faults, will be presented.

The second section of the report presents a compilation of all magnitude 3.0 or greater and/or Modified Mercalli intensity IV or greater earthquakes that have occurred within 200 mi (320 km) of the site. The relation of historical seismicity to known Quaternary faults and other features is discussed. The largest earthquake sequence occurring near the proposed site, the 1931 magnitude 6.4 Valentine, Texas, sequence, is discussed in greater detail. A significant earthquake sequence with magnitude > 7.0 mainshock occurring at a distance of 220 mi (354 km) from the study area is

23

also discussed, since it is also an example of the type of earthquakes that may be expected near the proposed site.

The third section of the report presents the results of seismic monitoring at the study area by University of Texas at El Paso personnel between July 12, 1988, and January 1, 1990. Equipment and field procedures used in the monitoring are discussed, and the rationale used in station siting is explained.

The final section of this report uses geologic information obtained from studies of Quaternary faults located near the site to evaluate the expected magnitudes and durations of earthquakes that might be expected along these faults in the future. This information is essential for designing a seismically safe repository.

TECTONIC SETTING

The Hueco Bolson is a basin that formed during extensional faulting that began 30 to 24 Ma ago (Seager et al., 1984). During this time, both Basin and Range faulting and faulting related to the development of the Rio Grande rift were underway, and it has been difficult to separate the southern Rio Grande rift from the southern Basin and Range physiographically or geologically throughout the southern New Mexico-West Texas-northern Chihuahua, Mexico, region (i.e., Gries, 1979).

An earlier deep sedimentary basin, the Chihuahua Trough, preceded the development of the Hueco Basin and other Quaternary-age basins of West Texas and Chihuahua (Henry and Price, 1985). The Chihuahua Trough began to form in the Jurassic Period, with continued deposition through the Cretaceous (Henry and Price, 1985). During Laramide deformation, Cretaceous rocks were thrust northeastward along a décollement zone composed of Jurassic evaporites, producing the thrust faults and folds found in the vicinity of the proposed low-level radioactive waste-disposal site.

The transition from compression to tension occurred about 30 Ma ago, and in southern New Mexico this early extension formed northwest-southeast-trending basins (Seager et al., 1984). The early phase of extension lasted until about 20 Ma ago and was followed by a period of relative quiescence. Extension picked up again about 8 Ma ago, but along north-south-trending faults in southern New Mexico (Seager et al., 1984). These north-south-trending faults bend in the El Paso area and follow the older northwest-southeast trends in West Texas and northeasternmost Chihuahua. Gravity and available seismic reflection data confirm the absence of north-south-trending structures in the proposed site.

Quaternary earthquake activity in West Texas has been significant, based on the presence of numerous Quaternary fault scarps and historic seismicity within the region (see next section). Recent studies (Machette, 1987; Sergent, Hauskins, and Beckwith, 1988) conclude that large scarps along the San Andres, Organ, and East Franklin Mountains in Texas and New Mexico and the Sierra San Jose del Prisco and Sierra de San Ignacio Mountains in Mexico are the result of earthquakes in the magnitude range of 7.0 to 7.5, with recurrence intervals as low as 5,000 years. Large scarps have also been recognized along both sides of the Rio Grande southeast of El Paso (for example, Seager and Morgan, 1979), along the Mayfield fault system south of Van Horn, and in the Salt Flat graben area (for example, Muehlberger et al., 1978). These scarps are located 16 to 90 mi (25 to 150 km) from the proposed site. The largest historic earthquake in Texas occurred along the Mayfield fault (Doser, 1987) (see next section).

A literature search for stress data from the region within a 200-mi (320-km) radius of the proposed site was conducted to determine how the stress information compares with the observed Quaternary faulting. Results of the search are shown in Figure 2 and listed in Table 1. The region within a 200-mi (320-km) radius of the proposed site is primarily within the southern Basin and Range/southern Rio Grande rift physiographic province. As stated previously, it is difficult to discern where the rift begins and the Basin and Range ends in this region using physiographic or geologic criteria, and not enough geophysical research has been done in the region to determine whether there are subsurface characteristics that can be used to divide the two provinces. The

southern Basin and Range/southern Rio Grande rift is characterized by block-type normal faulting of Quaternary age with alternating basins and mountain ranges, thin crust, and high heat flow.

A small portion of the study area lies within the Great Plains physiographic province (Figure 2). The Great Plains are characterized by thick crust, low heat flow, and no noted surface faulting of Quaternary age.

Stress indicators within the Rio Grande rift/Basin and Range province are derived from the alignment of dikes and cinder cones in recent (< 1 Ma) volcanic fields and a focal mechanism for the 1931 Valentine, Texas, earthquake. These indicators show that extension in the region is primarily oriented east-west to northwest-southeast and that the least compressive stress is generally much smaller in value than the intermediate principal stress. Thus, pure normal to oblique-normal faulting along north-south- to northeast-southwest-trending faults would be expected to occur.

Stress indicators within the Great Plains are derived from hydraulic fracture measurements and composite focal mechanisms of earthquakes occurring within an oil and gas field. These indicators show that extension in the region is oriented north-south to northeast-southwest and that the least compressive stress is much smaller in value. Therefore, normal faulting along east-west- to northwest-southeast-trending faults would be likely to occur in this region.

HISTORICAL SEISMICITY

Earthquakes with intensities of IV or greater or magnitudes of 3.0 or greater are listed in Table 2 and shown in Figure 3. The first step in compiling Table 2 was a computer search of epicenters compiled by the National Earthquake Information Center. Results of the search were cross checked against a list of earthquakes compiled by Sanford and Toppozada (1974), the bulletins and reports from the seismic observatory operated by New Mexico Institute of Mining and Technology in Socorro, New Mexico, and a list of earthquakes recorded by a network operating in the Permian Basin of West Texas between 1976 and 1979 (Keller et al., 1981).

Until the early 1960's, no seismograph stations were operated within the study area. As a result, most of the earthquakes that occurred before 1960 are poorly located, focal depths cannot be determined, and only earthquakes large enough to be recorded at distant stations or felt in a sparsely populated region have even been noted in historical records. We feel that the catalog of events listed in Table 2 prior to 1960 is only complete to the magnitude 4.5 to 5.0 level. Many smaller events probably occurred but were not detected by instruments or humans.

Since 1960, the number of seismograph stations operating in certain parts of the study area has increased (Figure 3), but the overall distribution of seismograph stations is insufficient to accurately locate earthquakes of magnitude < 4.0, and we still may not be detecting all earthquakes in the magnitude 3.0 to 3.5 range. Also, since a station must be located at a distance of no more than two focal depths from an earthquake to accurately determine the depth of the earthquake, the current station distribution does not allow for depth control.

Locating and detecting earthquakes within Chihuahua is extremely difficult, since seismographs have rarely operated within the state. In fact, we feel that the historical record for Chihuahua prior to 1960 is probably considerably less complete than that for the United States portion of the study area simply because earthquakes were not reported regularly unless they were large enough to be recorded or felt in the United States.

Because of the poor location accuracies (± 6 mi [10 km] or more) and lack of depth control for most earthquakes within the study area, it is not possible to conclusively link the earthquakes to specific mapped faults of Quaternary age. There do appear to be three major regions of seismic activity within the study area, however: a region near Valentine, Texas, associated with the Mayfield fault and the 1931 earthquake sequence, a region within the Permian Basin at the eastern edge of the study area, and northeastern Chihuahua.

Earthquakes within the Permian Basin correlate spatially with areas of oil field production and were not observed prior to the initiation of major secondary recovery operations in the area (Rogers and Malkiel, 1979). The largest magnitude earthquake observed within this portion of the

study area was 4.1, although earthquakes with magnitudes up to 5.0 (Harding, 1981) have been associated with oil production in other regions of West Texas.

In northeastern Chihuahua, where earthquakes of up to magnitude 5.0 have occurred, the geology is not well known. We have been unable to locate any maps that show faults with known Quaternary movement within this region. Consultations with a former University of Texas at El Paso faculty member who had done some reconnaissance fieldwork in the region confirmed a lack of obvious Quaternary faults, although he felt that the seismicity might possibly be occurring within a thick sequence of salt that has been observed at the surface in some parts of the region (R. Dyer, personal communication, 1987).

A third group of earthquakes is associated with the Mayfield fault near Valentine, Texas. In 1931 a sequence of large events occurred, including a felt foreshock, a mainshock of magnitude 6.4 (maximum intensity of VIII), and at least 4 aftershocks of intensity V. The isoseismal map of the mainshock (Figure 4) indicates that a Modified Mercalli intensity of V to VI may have been reached at the proposed site during this earthquake. All buildings in Valentine were damaged, and the earthquake was felt strongly enough in El Paso to alarm most citizens and cause the cracking of plaster on walls and ceilings (Sellards, 1933, cited in Davis et al., 1989). Had the area near the mainshock been more densely populated, severe damage and deaths may have occurred.

Waveform modeling of the mainshock (Doser, 1987) suggests that the earthquake occurred along the southern branch of the Mayfield fault, nucleating near a bend in the fault. The rupture began at a depth of 6 mi (10 km), was a complex rupture composed of at least three subevents, and caused about 8 to 10 inches (20 to 25 cm) of slip along the fault at depth. A study of geodetic data (Ni et al., 1981) suggested that as much as 4 inches (10 cm) of vertical movement may have occurred along the fault, in good agreement with the waveform modeling results. It is important to note that surface faulting was not observed along the Mayfield fault after the earthquake, suggesting that earthquakes of up to this magnitude could occur anywhere in the Trans-Pecos region and leave no surficial evidence of their occurrence. Geologic evidence (Muehlberger et al.,

1978) also suggests that the 1931 earthquake is not the largest possible event that could occur along the Mayfield fault.

An important sequence of earthquakes with a mainshock of magnitude ~ 7.2 that occurred just outside the bounds of the 200 mi (320 km) study area deserves mention, since it is also representative of the type of seismicity found within the southern Basin and Range/Rio Grande rift province. On May 3, 1887, a large earthquake occurred near Bavispe, northern Sonora (DuBois and Smith, 1980). The north end of the surface rupture was located about 5 mi (8 km) south of Douglas, Arizona. The surface fault trace was 30 mi (50 km) long, with an average surface displacement of 10 ft (3 m). Surface displacement was a combination of normal and right-lateral movement. A maximum normal displacement of 20 ft (6 m) was measured along some portions of the fault. The entire city of Bavispe was destroyed, and 51 people were killed. The Modified Mercalli intensity of the earthquake at Bavispe and surrounding areas of Arizona and Sonora reached XII (Figure 5). Although the earthquake was more distant from El Paso than the 1931 Valentine earthquake, it was felt more severely and caused more damage. Intensity in El Paso ranged from VII to VIII for the Sonora event. The isoseismal map (Figure 5) suggests that an intensity of V to VI may have been reached at the site, an intensity as severe as that from the Valentine earthquake (Figure 4). We feel that the Sonora earthquake is very representative of the type of earthquake that might occur on one of the major range bounding faults (East Franklin, East Organ, Amargosa faults) present in the region that includes the proposed site.

RESULTS OF SEISMIC MONITORING AT THE PROPOSED SITE

On July 12, 1988, a temporary network of seismograph stations consisting of three Sprengnether MEQ-800 smoked paper drum recorders with Mark Products L-4 seismometers was installed in the vicinity of the proposed site. Figure 6 shows the locations of the stations at Campo Grande Mountain (CGM), the northwest corner of the proposed disposal site (WDS), and along the main entry road to the site near the Campo Grande fault (FIN). A minimum of three stations is

needed to accurately locate an earthquake. The station configuration was designed to detect any seismicity associated with the segment of the Campo Grande fault nearest the proposed site. Temporary stations (squares, Figure 6) were placed far enough from roads to prevent vandalism and some road noise, but close enough to allow easy access for record changing. Only the Campo Grande Mountain station is located on bedrock, and consequently it has been our quietest station. The seismographs have been operating continuously since their installation. Records are changed and equipment checked every 4 days at the portable stations.

During the summer of 1989, we began installing a permanent network of stations (circles, Figure 6). These stations use Kinemetrics analog telemetry equipment in conjunction with the L-4 seismometers to radio telemeter data to a central receiving site on Campo Grande Mountain. The equipment is powered by batteries charged by solar collectors. Data from the central receiving site are then radioed to the seismic observatory on the University of Texas at El Paso campus, where they are recorded on thermal paper. Records at the observatory are changed every day. Since the permanent stations do not need routine maintenance, they may be located as much as 0.5 mi (0.8 km) from the temporary stations. Since September 15, 1989, the permanent station at Campo Grande Mountain (CGM2) has been operational; on March 9, 1990 the permanent station at the proposed site (WDSE) became operational and on March 23, 1990 the permanent station near the main entry road (FIN2) became operational.

Between July 12, 1988, and January 31, 1990, three local earthquakes were recorded (Table 3 and Figure 6). Copies of the seismograms are on file with the Texas Low-Level Radioactive Waste Disposal Authority. During the December 1988 and August 1988 events only two stations in the network were operating, so we could not locate the earthquakes at a specific point. The February 1989 event was too small to be recorded at CGM1, so it also is not well located. All three earthquakes had magnitudes of less than 1.0 and were not recorded at our permanent station on campus in El Paso. The February 1989 event is the only event that may have been associated with the Campo Grande fault. The December 1988 event may have been associated with the Amargosa fault.

The rate of seismic activity near the proposed site is surprisingly low. In the El Paso observatory we record about one local earthquake a month, and we were anticipating a similar rate near the study area; however, results to date suggest the rate of seismicity at the proposed site is one to two local earthquakes per year.

EXPECTED PARAMETERS OF EARTHQUAKES NEAR THE PROPOSED REPOSITORY SITE

Magnitudes and durations have been estimated from geologic information for earthquakes occurring at three locations near the proposed site: along the Campo Grande fault 1.8 mi (3 km) away, along the Amargosa fault in Mexico 15 mi (25 km) away, and directly beneath the proposed site along a fault that has not produced surface rupture in the past (and hence has not been mapped at the surface). The Campo Grande fault is the closest fault to the proposed site having documented Quaternary displacement, and the Amargosa fault is the closest major range-bounding fault to the proposed site.

Magnitudes for events along the Campo Grande and Amargosa faults were estimated using the magnitude-length and magnitude-displacement regression relationships developed by Slemmons et al. (1989) for dip-slip and strike-slip faults in extensional regimes. We considered several possibilities for rupture length and displacement along each fault.

For the Campo Grande fault we considered the possibility that the entire mapped fault (28 mi [45 km] long, Collins and Raney, 1989) ruptured and that only the segment of the fault that ruptured in the last earthquake (4 mi [7 km] long, Collins and Raney [1989]) ruptured. These rupture lengths led to magnitude estimates of 6.27 ± 0.29 (7 km rupture) and 7.02 ± 0.29 (45 km rupture) for an event along the fault. We also considered fault displacements per earthquake of 3 and 6 ft (1 and 2 m) (within the range of displacements suggested by Collins and Raney [1989] and Sergent, Hauskins, and Beckwith [1988]), which gave us magnitude estimates of 7.06 ± 0.35

31

(1 m displacement) and 7.40 ± 0.35 (2 m displacement). Thus the geologic record suggests that a magnitude 6.9 ± 0.41 earthquake occurred along the Campo Grande fault in Quaternary time.

The Amargosa fault has not been trenched or studied in great detail, so our estimates of fault length and displacement per earthquake on this fault are cruder. The entire fault appears to be 35 mi (57 km) long, so we assumed that it ruptured in one event, although fault ruptures of this length for events in the western Cordillera of the United States are very rare (Doser and Smith, 1989). This fault length gave us a magnitude estimate of 7.11 ± 0.29. In considering displacement per event we considered two extremes, the first being that the entire 23-ft - (7-m-) high scarp observed in the field occurred during one event, the second that 6 ft (2 m) of displacement (an average value for large western Cordillera earthquakes, Doser and Smith [1989]) occurred per event. It should be noted that a maximum displacement of 23 ft (7 m) has only been observed for one event in the entire western Cordillera (at Hebgen Lake, Montana, in 1959). Using these displacement values, the relation of Slemmons et al. predicts magnitudes of 9.1 ± 0.35 (7 m displacement) and 7.40 ± 0.35 (2 m displacement). A magnitude of 9.1 is certainly not credible, leading us to doubt the 23-ft (7-m) displacement value. Therefore the geologic record suggests that a magnitude 7.26 ± 0.15 earthquake occurred on the Amargosa fault in Quaternary time.

The third event we considered was one occurring directly beneath the proposed site (0 km), producing no surface rupture. We term such an earthquake a "background event." The magnitude 6.4 Valentine earthquake did not produce surface faulting. Earthquakes in the western Cordillera with magnitudes as great as 6.6 have not produced surface faulting, but earthquakes with magnitudes of 6.2 occasionally produce surface faulting. Studies of other western Cordillera earthquakes (Doser & Smith, 1989) suggests a background event of 6.4 ± 0.1 could occur anywhere on the site.

The above magnitude estimates were used to estimate the duration of shaking (when horizontal accelerations would be greater than or equal to 0.05 g [1 g = acceleration of gravity, 980 cm/(sec × sec)]) at the site using the relationships of Krinitzsky et al. (1988). A discussion of peak horizontal acceleration and velocities is found in a separate report. We used the relationship of

Krinitzsky et al., which was developed for hard sites (solid rock and stiff soil) and shallow (<19 km deep) earthquakes, since testing of near-surface materials at the site has indicated that the materials are stiff (Nazarian and Yuan, 1989) and earthquakes like the 1931 Valentine event have been shallow. We assumed an earthquake on the Campo Grande fault would be 1.8 mi (3 km) from the site and an earthquake on the Amargosa fault would be 15 mi (25 km) from the site. The relationship of Krinitzsky et al. does not hold when the distance to the event is 0 km, so we assumed that the background event was located 0.6 mi (1 km) from the proposed site. For the Campo Grande fault, duration of shaking estimates ranged from 1.51 sec (magnitude 6.27 event) to 4.63 sec (magnitude 7.40 event) with an average duration of 3.15 ± 1.10 sec. Duration of shaking estimates for the Amargosa fault ranged from 6.57 sec (magnitude 7.11 event) to 8.75 sec (magnitude 7.40 event) with a mean duration of 7.66 ± 1.09 sec. Duration estimates for a background event were 1.12 sec (magnitude 6.3 event) to 1.36 sec (magnitude 6.5 event) (1.24 ± 0.12 sec average). These values suggest that although an earthquake on the Amargosa fault would be farther from the site, the duration of shaking at the site from an event on the Amargosa fault could be 1.4 to 5.8 times longer than from an earthquake on the Campo Grande fault.

It should be noted that the relationships used to estimate magnitude and duration represent averages of many earthquakes. The position of the study area with respect to the direction of rupture during an earthquake would strongly influence the duration. Also, most relationships are derived using data recorded at distances greater than 6 mi (10 km) from an earthquake, so it is uncertain how well the relationships predict duration very close to a fault.

CONCLUSIONS

Previous studies have shown that Quaternary faulting, primarily with normal dip-slip movement, is common throughout Trans-Pecos Texas. Stress orientations as determined from studies of geologic features and earthquakes confirm that normal faulting is continuing within the region.

A study of the historical seismicity of the region within a 200-mi (320-km) radius of the proposed site indicates that there has been a moderate level of earthquake activity. The three major areas of seismicity in this region are the oil and gas fields of the Permian Basin, the region near the Mayfield fault, site of the 1931 Valentine earthquake, and a region of Chihuahua 50 to 100 mi (80 to 160 km) south of the study area. The largest earthquake within the region, the 1931 mainshock, did not rupture the ground surface; however, a magnitude ~ 7.2 event in 1887 produced extensive ground rupture and damage approximately 200 mi (320 km) from the proposed site. The 1887 event is a good example of the type of earthquake that might be expected to occur along the Amargosa fault located 15 mi (25 km) from the proposed site. The Valentine earthquake (magnitude 6.4) represents a background event that might be expected to occur anywhere within the region, even directly beneath the study area, and leave no surficial geologic expression of its occurrence.

Earthquake monitoring at the study area shows an extremely low level of activity, only three earthquakes in an 21-month period. Only one of the earthquakes could be associated with the Campo Grande fault. The low level of seismicity does not in any way indicate that faults near the proposed site are "dead." For at least two decades before the 1983 Borah Peak, Idaho, earthquake (magnitude 7.0) the region within 15 mi (25 km) of the mainshock epicenter was quiescent at the magnitude > 3.5 level (Dewey, 1985).

The geologic record of surface faulting indicates that earthquakes with magnitudes of up to 7.4 have occurred on the Campo Grande and Amargosa faults. A background event of up to magnitude 6.5, producing no surface rupture, might also occur within the vicinity of the proposed site. Although a large earthquake along the Amargosa fault is farther from the proposed site, it would produce the greatest duration of shaking. Any waste repository built at the proposed site should be capable of withstanding the duration of shaking from a large earthquake (up to 8.8 sec) along the Amargosa fault.

REFERENCES

Balk, R., 1962, Geologic map and sections of Tres Hermanas Mountains: New Mexico Bureau of Mines and Mineral Resources Geological Map 16.

Collins, E. W., and Raney, J. A., 1989, Description and Quaternary history of the Campo Grande fault of the Hueco Basin, Hudspeth and El Paso Counties, Trans-Pecos Texas: The University of Texas at Austin, Bureau of Economic Geology, report prepared for Texas Low-Level Radioactive Waste Disposal Authority under Interagency Contract Number IAC(88-89)0932.

Dewey, J. W., 1985, Instrumental seismicity of central Idaho: U.S. Geological Survey Open-File Report 85-290, p. 264–284.

Doser, D. I., 1987, The August 1931 Valentine, Texas, earthquake: evidence for normal faulting in West Texas: Bulletin of the Seismological Society of America, v. 77, p. 2005–2017.

Doser, D. I., and Smith, R. B., 1989, An assessment of source parameters of earthquakes in the cordillera of the western United States: Bulletin of the Seismological Society of America, v. 79, p. 1383–1409.

Doser, D. I., Baker, M. R., and Mason, D. B., in preparation, Seismicity in the War-Wink gas field, Delaware Basin, West Texas, and its relationship to petroleum production.

DuBois, S. M., and Smith, A. W., 1980, The 1887 earthquake in San Bernardino Valley, Sonora: State of Arizona Bureau of Geology and Mining Technology, Special Paper Number 3, 112 p.

Gries, J. C., 1979, Problems of delineation of the Rio Grande rift into the Chihuahua tectonic belt of northern Mexico, *in* R. E. Riecker, ed., Rio Grande rift: tectonics and magmatism, American Geophysical Union Special Publication, p. 107–113.

Harding, S. T., 1981, Induced seismicity in Cogdell Canyon Reef oil field: U.S. Geological Survey Open-File Report 81-167, p. 451–455.

Henry, C. D., and Price, J. G., 1985, Summary of the tectonic development of Trans-Pecos Texas: The University of Texas at Austin, Bureau of Economic Geology Miscellaneous Map No. 36, scale 1:500,000, 8 p.

Hoffer, J. M., 1976, The Potrillo basalt field, south-central New Mexico; Cenozoic volcanism in southwestern New Mexico: New Mexico Geological Society, Special Publication No. 5, p. 89-92.

Keller, G. R., Rogers, A. M., Lund, R. J., and Orr, C. D., 1981, A seismicity and seismotectonic study of the Kermit seismic zone, Texas: U.S. Geological Survey Open-File Report 81-37, 383 p.

Krinitzsky, E. L., Chang, F. K., and Nuttli, O. W., 1988, Magnitude-related earthquake ground motions: Bulletin of the Association of Engineering Geologists, v. 25, no. 4, p. 399–423.

Machette, M. N., 1987, Preliminary assessment of paleoseismicity at White Sands Missile Range, southern New Mexico: Evidence for recency of faulting, fault segmentation, and repeat intervals for major earthquakes in the region: U. S. Geological Survey Open-File Report 87-444, 46 p.

Muehlberger, W. R., Belcher, R. C., and Goetz, L. K., 1978, Quaternary faulting in Trans-Pecos Texas: Geology, v. 6, no. 6, p. 337–340.

Nazarian, S., and Yuan, D-R., 1989, Near-surface profiling of proposed location for Texas low-level radioactive waste disposal facility: Austin, Texas, report prepared for The University of Texas at Austin, Bureau of Economic Geology and Texas Low-Level Radioactive Waste Disposal Authority, research report number 89-3.

Ni, J. F., Reilinger, R. E., and Brown, L. D., 1981, Vertical crustal movements in the vicinity of the 1931 Valentine, Texas, earthquake: Bulletin of the Seismological Society of America, v. 71, p. 857–864.

Rogers, A. M., and Malkiel, A., 1979, A study of earthquakes in the Permian Basin of Texas-New Mexico: Bulletin of the Seismological Society of America, v. 69, p. 843–865.

Sanford, A. R., and Toppozada, T. R., 1974, Seismicity of proposed radioactive waste disposal site in southeastern New Mexico: New Mexico Bureau of Mines and Mineral Resources Circular 143, 15 p.

Sanford, A. R., Olsen, K. H., and Jaksha, L. H., 1981, Earthquakes in New Mexico, 1849-1977: New Mexico Bureau of Mines and Mineral Resources Circular 171, 19 p.

Seager, W. R., and Morgan, R., 1979, Rio Grande rift in southern New Mexico, west Texas, and northern Chihuahua, *in* Reicker, R. E., ed., Rio Grande rift: tectonics and magmatism: American Geophysical Union Special Publication, p. 87–106.

Seager, W. R., Shafiqullah, M., Hawley, J. W., and Marvin, R. F., 1984, New K-Ar dates from basalts and the evolution of the southern Rio Grande rift: Geological Society of America Bulletin, v. 95, no. 1, p. 87–99.

Sellards, E. H., 1933, The Valentine, Texas, earthquake: University of Texas Bulletin No. 3201, p. 113–138.

Sergent, Hauskins, and Beckwith, consulting geotechnical engineers, 1988, Preliminary geologic and hydrologic evaluation of the Fort Hancock site (NTP-S34), Hudspeth County, Texas, for the disposal of low-level radioactive waste: SHB Job No. E88-4008B prepared for Hudspeth County, Texas, Hudspeth County Conservation and Reclamation District No. 1, Hudspeth County Underground Water Conservation District No. 1, and El Paso County, Texas.

Slemmons, D. B., Bodin, P., and Zhang, X., 1989, Determination of earthquake size from surface faulting events: Proceedings of International Seminar on Seismic Zonation, Guangszhou, China.

Weber, R. H., 1964, Geology of the Carrizozo Quadrangle, New Mexico: New Mexico Geological Society Field Conference Guidebook 15, p. 100–109.

Woodward, L. A., Callender, J. F., Seager, W. F., Chapin, C. E., Gries, J. C., Shaffer, W. L., and Zilinski, R. E., 1978, Tectonic map of Rio Grande rift region in New Mexico,

Chihuahua, and Texas, *in* Hawley, J. W., ed., Guidebook to Rio Grande rift in New Mexico and Colorado: New Mexico Bureau of Mines and Mineral Resources Circular 163.

Zemanek, J. E., Bleen, E., Norton, L. J., and Caldwell, R. L., 1970, Formation evaluation by inspection with the borehole televiewer: Geophysics, v. 35, no. 2, p. 254–269.
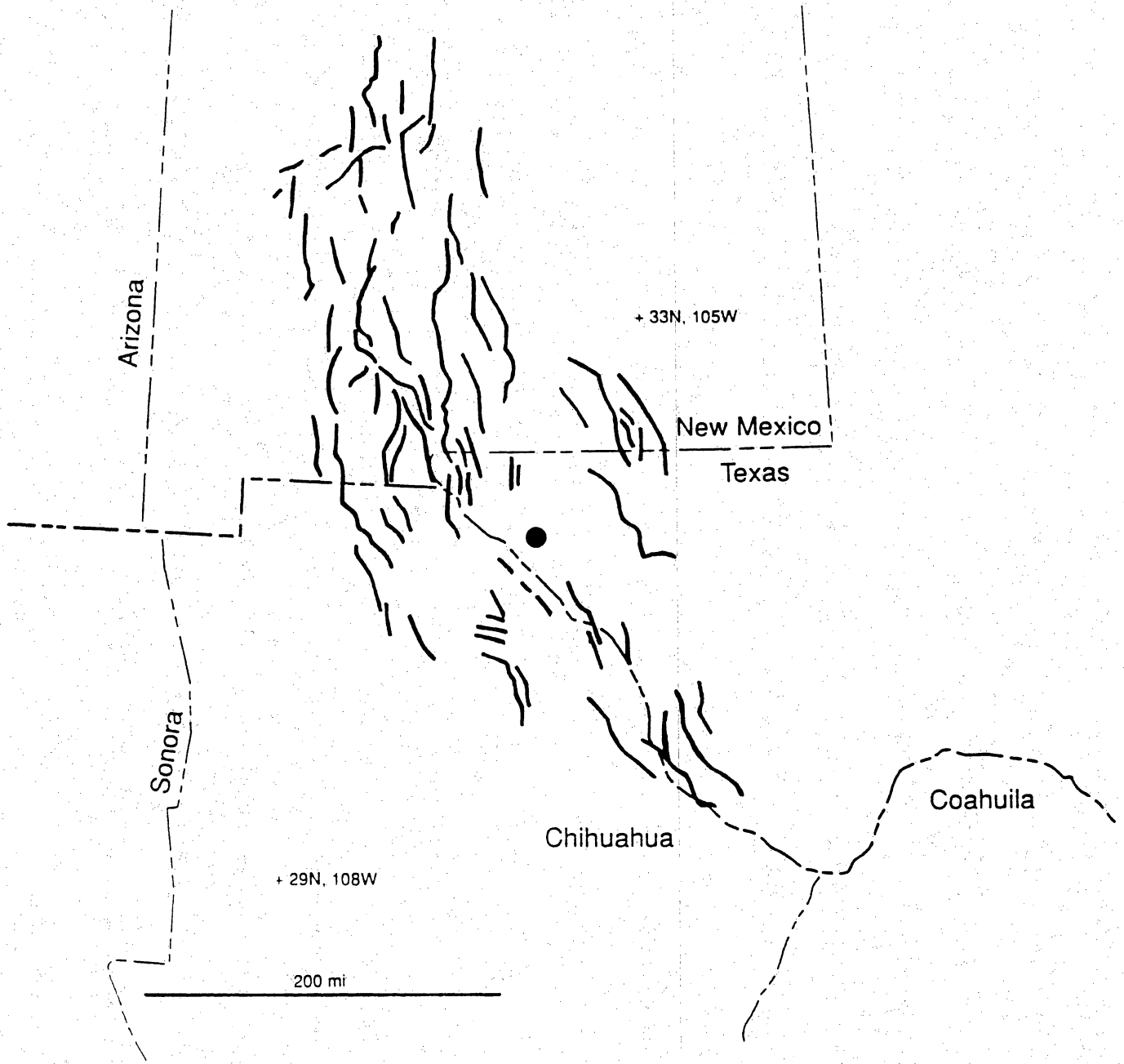
Figure 1. Index map showing Cenozoic faults (bold lines) in the vicinity of the proposed low-level radioactive waste repository site (dot). Faults are modified from Woodward et al. (1978).
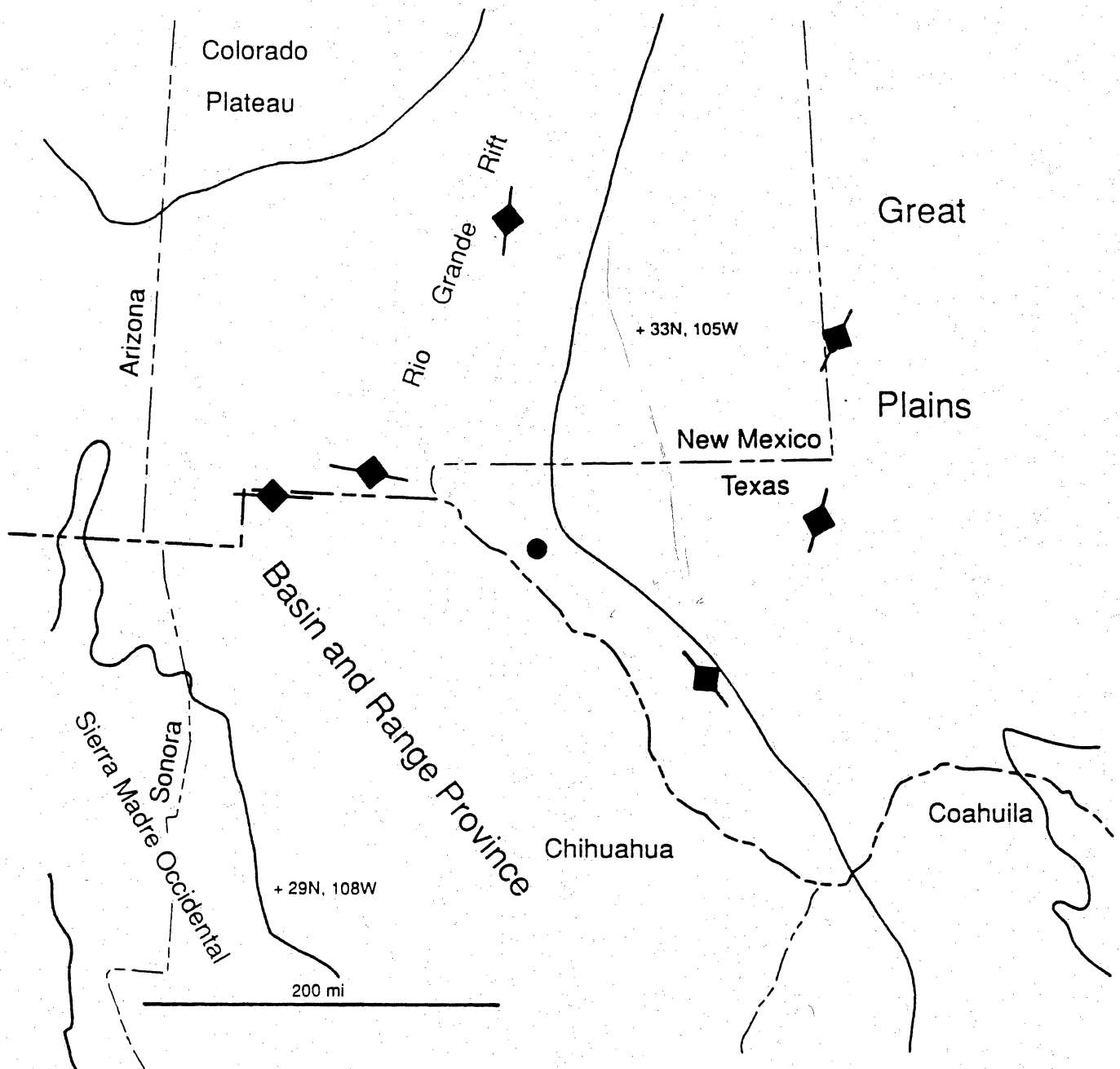
Figure 2. Physiographic provinces and the location of stress indicators (diamonds) within a 200-mi (320-km) radius of the proposed low-level radioactive waste repository site (dot). Datum is sea level. Lines drawn through stress indicator locations show the orientation of the least compressive stress direction (see Table 1).

41
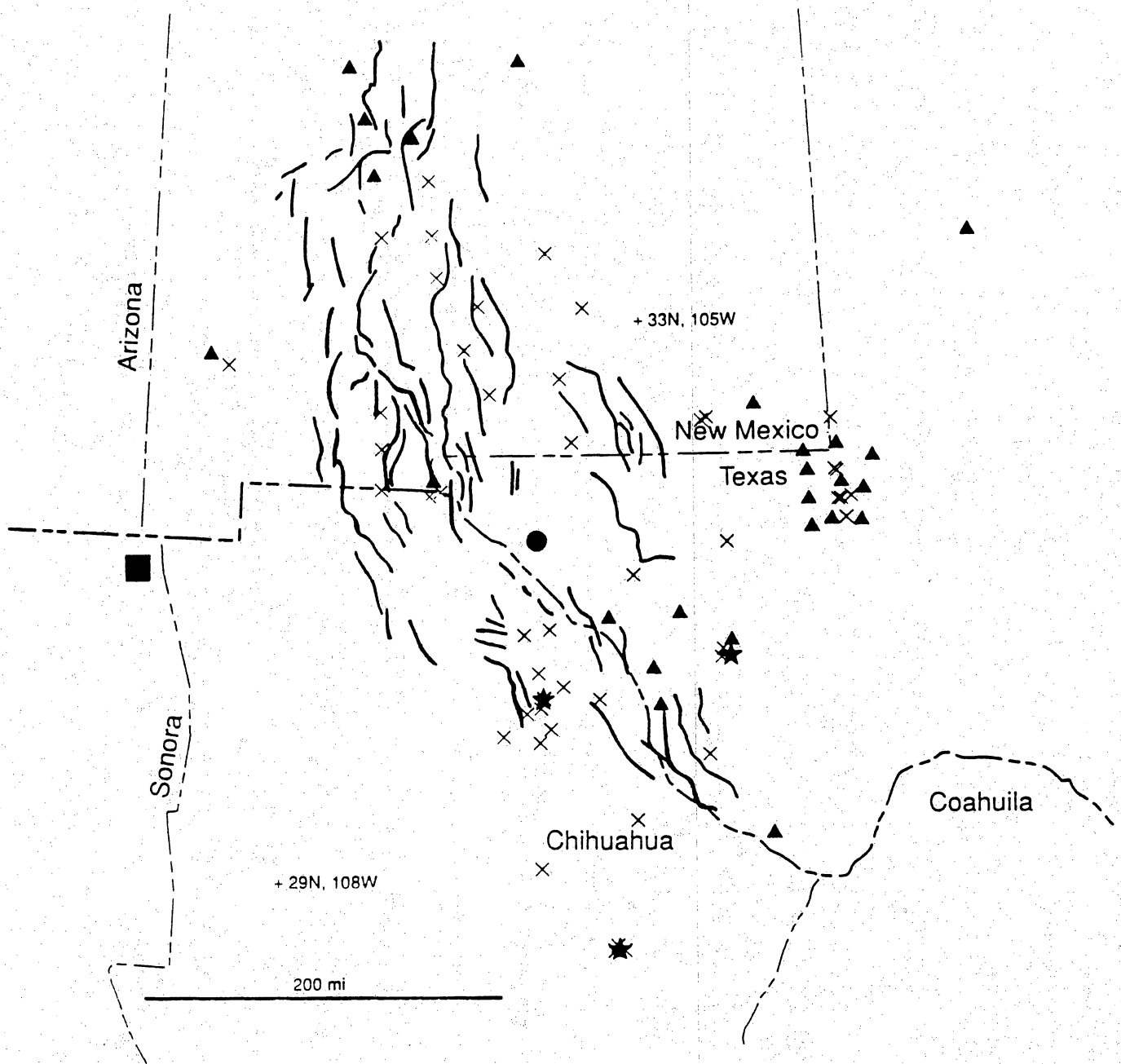
Figure 3. Historical seismicity with magnitudes greater than or equal to 3.0 and/or Modified Mercalli intensities greater than or equal to IV located within 200 mi (320 km) of the proposed low-level radioactive waste repository site (dot). Individual locations and origin times are given in Table 2. Faults (bold lines) are taken from Figure 1. Stars are magnitude 5.0 or greater earthquakes, x's are magnitude < 5.0 earthquakes, triangles are seismograph stations operating continuously for more than 1 year between 1960 and 1988, and the square is the location of the 1887 Sonora earthquake.

42
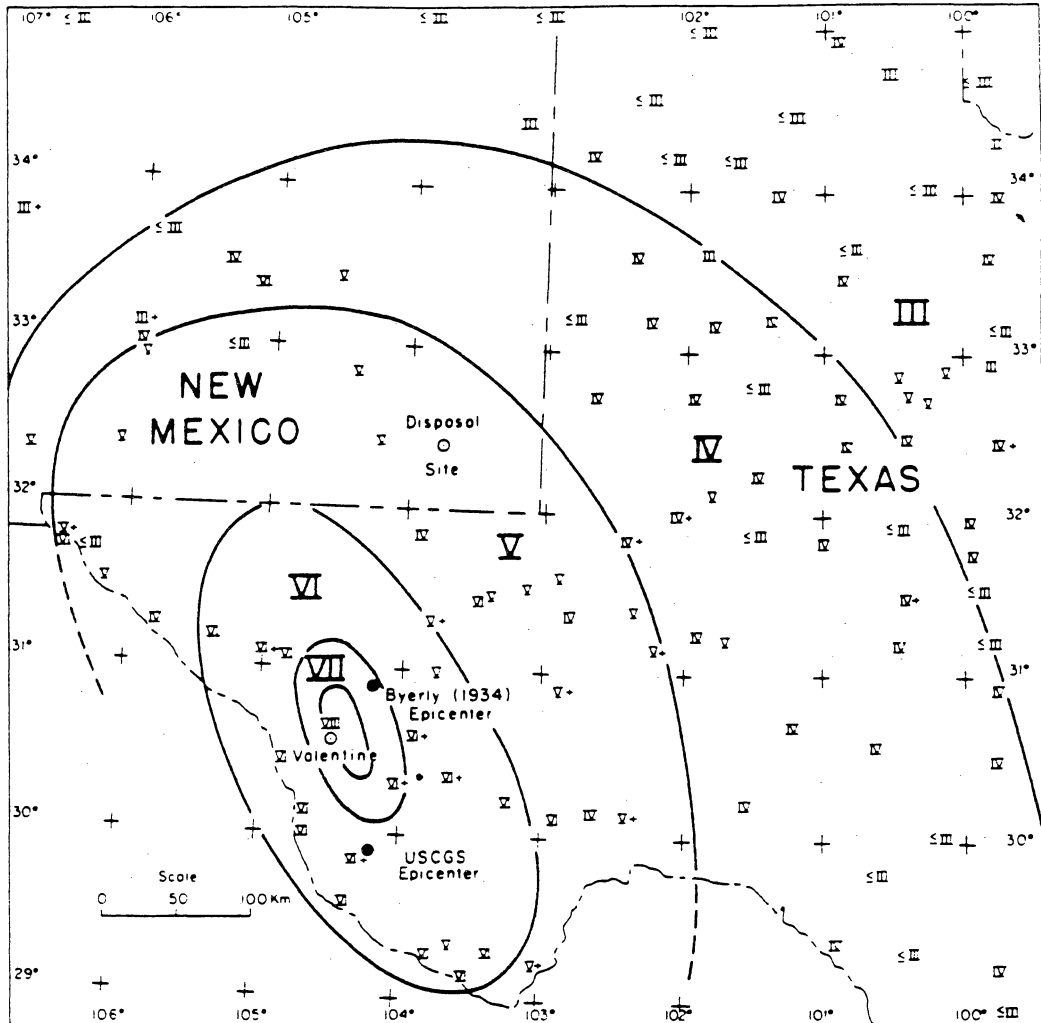
Figure 4. Isoseismal map showing Modified Mercalli intensities for the August 16, 1931, Valentine, Texas, earthquake. Modified from Sanford and Toppozada (1974). Proposed low-level radioactive waste repository site is indicated by a square.

43
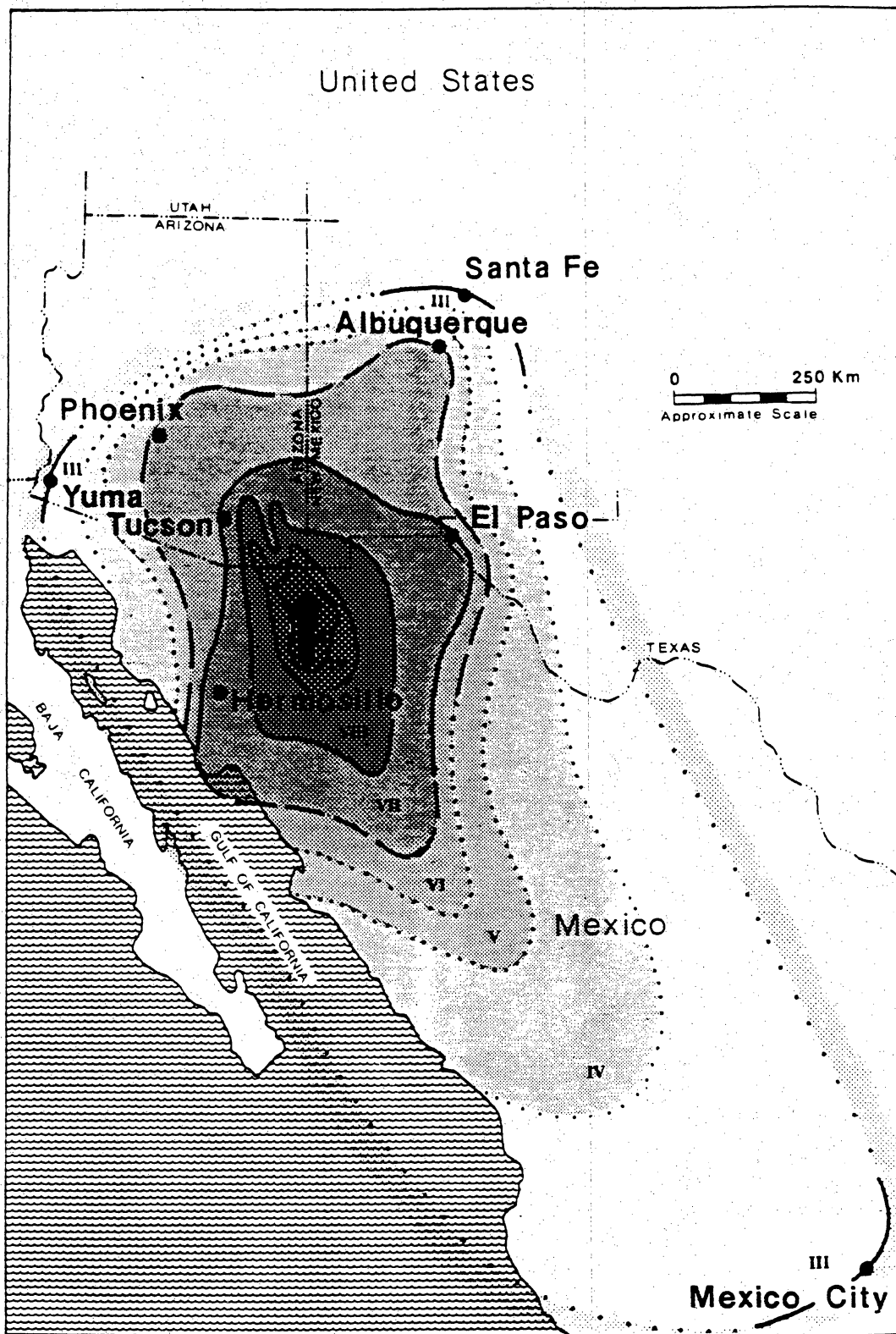
Figure 5. Isoseismal map showing Modified Mercalli intensities for the May 3, 1887, Sonora earthquake. Modified from DuBois and Smith (1980). Proposed low-level radioactive waste repository site is indicated by a square.
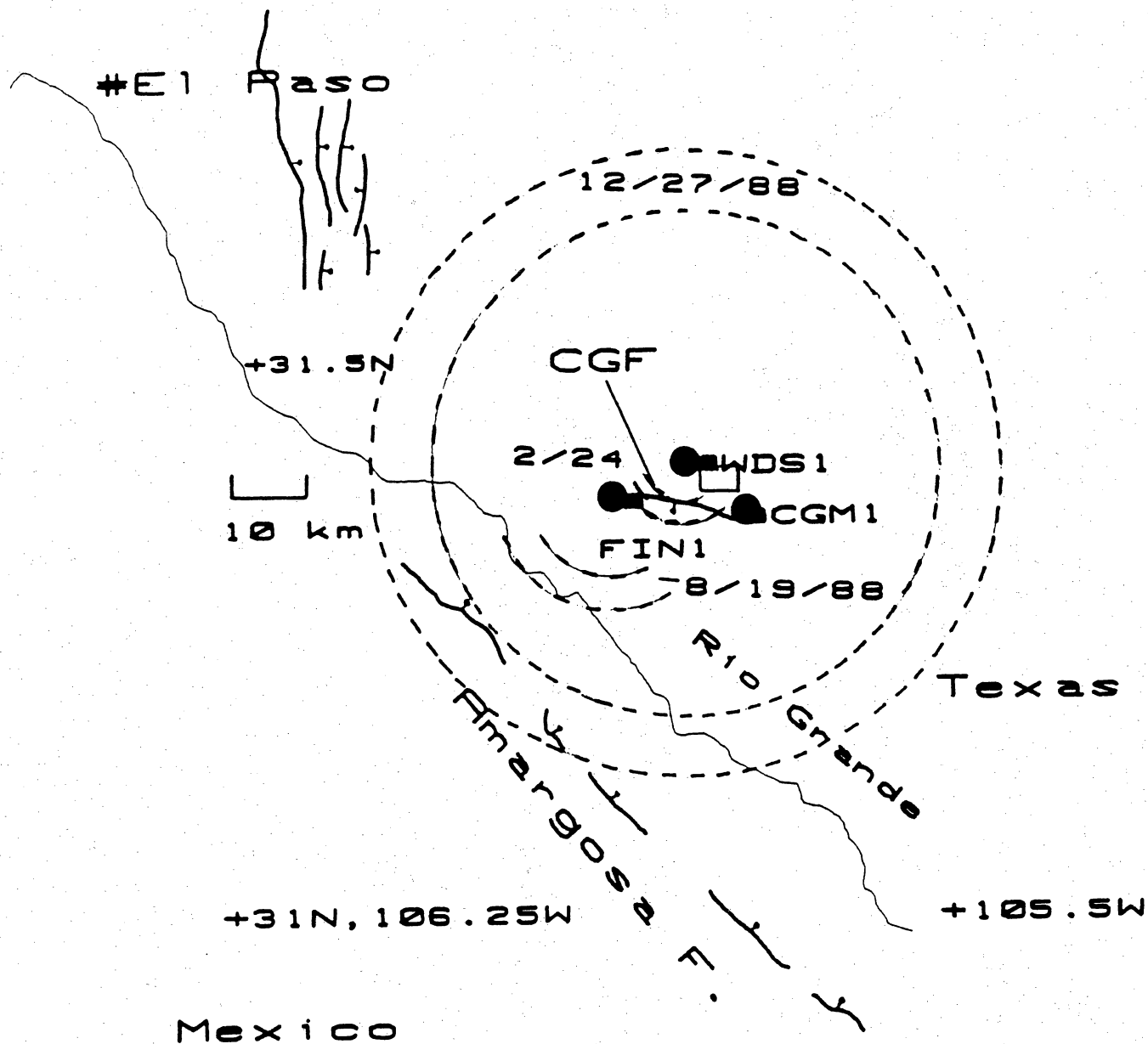
Figure 6. Major Quaternary faults (bold lines) located near proposed low-level radioactive waste repository site. Approximate boundary of the proposed site is indicated by a rectangle. Temporary stations operating are indicated by squares, permanent stations by dots. Earthquake locations shown were recorded by the seismograph network between July 1988 and January 1990. Faults are taken from Henry and Price (1985) and Collins and Raney (1989). Balls on faults represent downthrown side of faults. CGF=Campo Grande fault, WDS=waste disposal site (proposed low-level radioactive waste repository site) seismograph station locations, CGM=Campo Grande Mountain seismograph station locations, FIN=Campo Grande fault seismograph station locations.

45

REGIONAL GEOPHYSICS AND GRAVITY SURVEY IN THE VICINITY OF

THE PROPOSED LOW-LEVEL RADIOACTIVE WASTE REPOSITORY,

HUDSPETH COUNTY, TEXAS

G. R. Keller

Department of Geological Sciences

The University of Texas at El Paso

INTRODUCTION

Analysis of measurements of the Earth's gravity field is a cost-effective way to obtain a generalized picture of subsurface structure. The measurements are straightforward, and the data processing techniques are well established and standardized. In the processing, known variations in the gravity field (such as the decrease with increasing elevation) are accounted for, leaving only variations (anomalies) that have geological significance. The interpretations of these measurements are non-unique in that it is theoretically possible for a variety of structures to produce the same pattern of anomalies. However, with the aid of other constraints such as drill-hole data, surface geologic mapping, and seismic surveys, gravity data are particularly useful in extrapolating a combined data base into an areal picture. This is the approach used in this study.

REGIONAL OVERVIEW

The pre-Cenozoic geologic history of West Texas is complex (e.g., Henry and Price, 1985) and is of much interest to researchers, petroleum geologists, and economic geologists, but it is of less direct importance to the evaluation of the proposed site for the low-level radioactive waste repository. However, one older feature of interest is the Clint fault (Upoff, 1978). This feature

was identified from deep drill holes just west of the El Paso–Hudspeth County line. Upoff (1978) demonstrated that this subsurface feature was active in the Cretaceous, probably as a fault with a component of down-to-the-south normal displacement. However, a strike-slip component of movement is possible. This fault occurs along a northwest-southeast-trending gravity gradient that extends southeastward toward the Campo Grande fault zone. The Campo Grande fault has experienced major movements in the late Cenozoic, indicating reactivation by extension related to the Rio Grande rift. Thus it is possible that the Campo Grande fault zone is a reactivated fault related to the Mesozoic system of faults that includes the Clint fault.

The Rio Grande rift (Figure 1) extension is responsible for the modern tectonic activity in far West Texas. This major continental rift zone extends from Central Colorado southward into West Texas and northern Mexico. This feature has had a two-phase history beginning about 30 MA (e.g., Seager et al., 1984; Morgan et al., 1986; Keller et al., 1990). The first phase, as seen in New Mexico, involved northwest-southeast-trending, low-angle normal faults, and was accompanied by the eruption of large volumes of basaltic andesites and some rhyolite. After a lull in the Miocene, the second phase of rifting began at about 10 Ma and continues today. It was characterized by high-angle faulting and, in New Mexico, minor amounts of basaltic volcanism. From El Paso northward, the faulting was generally north-south trending, but these structures were deflected southeastward at El Paso (Figure 2) to form the southern Hueco Bolson. The bolson's northeastern (Campo Grande fault) and southwestern (Amargosa fault) boundaries were active at this time.

Heat flow associated with the Rio Grande rift is generally high (Figure 3) but has a complex distribution due to ground-water flow in the basins. The areas of highest heat flow generally correlate with the regions were seismic and gravity data indicate the crust is thinnest (Figure 4) (Sinno et al., 1986; Daggett et al., 1986; Keller et al., 1990). In addition to this evidence for active crustal-scale deformation, minor seismic activity is associated with the Rio Grande rift (see accompanying discussion by Doser), and there is evidence for contemporary vertical crustal movements in central New Mexico (Larsen et al., 1986) and west Texas (Reilinger et al., 1980; Ni

et al., 1981). Reilinger et al. (1980) suggested that the Diablo Plateau may have experienced 19 ± 3cm of relative uplift with respect to the Salt Flat graben between 1934 and 1977. This possible evidence of uplift, young fault scarps in the Salt Flat graben (Muehlberger et al., 1978), and the crustal structure anomalies in the Diablo Plateau area (Daggett et al., 1986) suggest that zones of extension related to the Rio Grande rift may be present as far east as the Salt Flat graben.

The Hueco Bolson is a major basin of the Rio Grande rift. However, our knowledge of its deep structure is based on seismic refraction surveys in the El Paso area (Mattick, 1967); a few deep drill holes (Upoff, 1978), and gravity data (Wen, 1983). Wen (1983) used a combination of drilling data and analysis of gravity anomalies to estimate bolson fill thicknesses in the area and his map is shown as Figure 5. Fill exceeds 2 km in thickness in several areas including the region southwest of the proposed repository. A more detailed geophysical analysis of the proposed repository area was undertaken to further evaluate its deep structure.

GRAVITY SURVEYS AND DATA PROCESSING

The University of Texas at El Paso maintains a large data base of gravity readings from West Texas and surrounding areas that provides a general picture of regional structure. The gravity anomaly map shown in Figure 6 depicts a large gravity low in the area of the Hueco Bolson that approximately maps the infilling sedimentary rocks (i.e., the more negative the gravity anomaly the thicker the sedimentary rocks). Mountain ranges that bound the bolson are associated with gravity highs. The large, north-south-trending gravity high in the eastern portion of the Diablo Plateau is due to a deep-seated structure (Daggett et al., 1986).

Evaluation of the proposed site for the low-level radioactive waste repository required a more detailed analysis than the existing gravity data could provide. Thus, additional gravity surveys were undertaken. A profile of gravity measurements was made along a county road from Fort Hancock into the area of the proposed repository. Readings were also taken along all of the seismic lines recorded by Phillips et al. (1986), and at accessible benchmarks and other topographic control

points. These data made it possible to identify a few key areas where additional measurements were made.

All measurements were combined into a computerized data base and processed to construct the gravity anomaly map shown in Figure 7. Reduction of the measurements to Bouguer anomaly values employed the equations of Cordell et al. (1982), which are the standard equations used by the U.S. Geological Survey. The usual datum of sea level was chosen. Because of the relatively low density of rocks in the site area, a reduction density of 2.4 gm/cc was employed. All readings were tied to the international network (Morelli, 1976) gravity base station on the campus of The University of Texas at El Paso. A LaCoste-Romberg gravity meter (no. 720) was used for all readings. The map shown in Figure 7 was constructed by first gridding the gravity values employing the technique of minimum curvature (Briggs, 1974) and then contouring the grid using the computer technique of Sampson (1978). Locations for all gravity measurements are shown in Figure 7. A profile of anomaly values from Fort Hancock to the study area was also plotted (Figure 8); the closely spaced stations comprising this profile are evident on Figure 7.

INTERPRETATION

Several features are evident in Figures 7 and 8, and a portion of the trace of the Campo Grande fault and Campo Grande Mountain is included in Figure 7 for location purposes. A high gradient associated with the trace of the Campo Grande fault documents that the thickness of the bolson deposits abruptly increases southwest of the fault. A fault would be inferred near this gradient if one were not already known to exist at this location. The magnitude of this gradient establishes that the Campo Grande fault is a major deep-seated feature whose movement is down-to-the-southwest. The decrease in this gradient southeastward toward Campo Grande Mountain indicates that the throw on this fault decreases southeastward.

As one approaches the study area from the Campo Grande fault, the anomaly values reach a plateau at about -150 milligals and then decline. This plateau correlates well with the limited areas

where bedrock is known to be shallow and thus can be used to infer the extent of shallow bedrock. The low values north of this plateau can be interpreted to delineate a small basin in this area. However, as discussed below, thickening of Cretaceous rocks also contributes to this anomaly. The proposed repository site appears to be contained within this inferred basin. The pattern of contours indicates that this basin extends southeastward toward Campo Grande Mountain, but the gravity anomalies do not correlate well with known bedrock depths, indicating the presence of a deeper structure.

The final step in the gravity analysis was to construct an integrated Earth model along the gravity profile extending from Fort Hancock through the study area. The resulting model shown in Figure 8 should be considered to be a generalized geologic cross-section because it is constrained by both drilling and seismic data. For the purpose of this model, basement (density = 2.7 gm/cc) was all Pre-Cretaceous rocks. South of the Campo Grande fault, the bolson fill was assigned a density of 2.35 gm/cc in accord with the regional density contrast value established by Wen (1983); north of this fault, a lower value (2.2 gm/cc) was used because the fill was relatively thin (and thus not as compacted) and mostly unsaturated. Cretaceous rocks were assigned a density of 2.5 gm/cc based on previous analyses of these rocks in west Texas (summarized in Keller et al., 1985). The model shows the fill thickening abruptly southwest of the Campo Grande fault. The structurally high block just north of this fault involves the basement. Because of the known shallow structure, this basement high is probably not due to Rio Grande rift related normal faulting. Its presence is consistent with the idea that the Campo Grande fault may have a history of pre-rift movement. A small component of strike slip movement could produce such a feature. There are several mid-Cenozoic intrusions in the area (Quitman Mountains, Finlay Mountains, and Hueco Tanks) and it is interesting to speculate that one of these pre-rifting intrusions used the Campo Grande fault as a conduit. The basin geometry shown north of the structural high is consistent with both seismic reflection (see accompanying discussion by Baker) and drilling results. The gravity low in this area could not be modeled with bolson fill thickness variations alone. A thickening of Cretaceous units had to be included. The zone of maximum thickening at

51

13 km (Figure 8) coincides approximately with the most northerly thrust fault in Cretaceous rocks recognized in the seismic data. Thus, thrust loading may have played some role in producing this gravity low. The northern end of the model depicts thinning of both Cretaceous and bolson fill units as the Diablo Plateau is approached.

REFERENCES

Daggett, P. H., Keller, G. R., Morgan, P., and Wen, C. L., 1986, Structure of the southern Rio Grande rift from gravity interpretation: Journal of Geophysical Research, v. 91, p. 6157–6167.

Decker, E. R., and Smithson, S. B., 1975, Heat flow and gravity interpretation across the Rio Grande rift in southern New Mexico and West Texas: Journal of Geophysical Research, v. 80, p. 2542–2552.

Keller, G. R., Morgan, P., and Seager, W. R., 1990, Crustal structure, gravity anomalies and heat flow in the southern Rio Grande rift and their relationship to extensional tectonics: Tectonophysics, v. 174, p. 21–37.

Larsen, S. C., Reilinger, R. E., and Brown, L., 1986, Evidence of ongoing crustal deformation related to magmatic activity near Socorro, New Mexico: Journal of Geophysical Research, v. 91, p. 6283–6292.

Mattick, R. E., 1967, A seismic and gravity profile across the Hueco Bolson, Texas: U. S. Geological Survey Professional Paper 575-D, p. 85–91.

Morgan, P., Seager, W. R., and Golombek, M. P., 1986, Cenozoic thermal, mechanical, and tectonic evolution of the Rio Grande rift: Journal of Geophysical Research, v. 91, p. 6263–6276.

Muehlberger, W. R., Belcher, R. C., and Goetz, L. K., 1978, Quaternary faulting in Trans-Pecos Texas: Geology, v. 6, p. 337–340.

Ni, J. F., Reilinger, R. E., and Brown, L. D., 1981, Vertical crustal movements in the vicinity of the 1931 Valentine, Texas, earthquake: Bulletin of the Seismological Society of America, v. 71, p. 857–864.

Reilinger, R. E., Brown, L., and Powers, D., 1980, New evidence for tectonic uplift in the Diablo Plateau region, West Texas: Geophysical Research Letters, v. 7, p. 181–184.

Reiter, M., Eggleston, R. E., Broadwell, B. R., and Minier, J., 1986, Terrestrial heat flow estimates from deep petroleum tests along the Rio Grande rift in central and southern New Mexico, *in* Riecker, R. E., ed., Rio Grande Rift: Tectonics and Magmatism: American Geophysical Union Special Publication, p. 253–267.

Seager, W. R., and Morgan, P., 1979, Rio Grande rift in southern new Mexico, West Texas, and northern Chihuahua, *in* Riecker, R. E., ed., Rio Grande Rift: Tectonics and Magmatism: American Geophysical Union Special Publication, p. 87–106.

Seager, W. R., Shafiqullah, M., Hawley, J. W., and Marvin, R., 1984, New K-Ar dates from basalts and the evolution of the southern Rio Grande rift: Geological Society of America Bulletin, v. 95, p. 87–99.

Sinno, Y. A., Daggett, P. H., Keller, G. R., Morgan, P., and Harder, S. H., 1986, Crustal structure of the southern Rio Grande rift determined from seismic refraction profiling: Journal of Geophysical Research, v. 91, p. 6143–6156.

Swanberg, C. A., 1979, Chemistry of thermal and non-thermal groundwaters in the Rio Grande rift and adjacent tectonic provinces, *in* Riecker, R. E., ed., Rio Grande Rift: Tectonics and Magmatism: American Geophysical Union Special Publication, p. 279–288.

Upoff, T. L., 1978, Subsurface stratigraphy and structure of the Mesilla and Hueco bolsons, El Paso region, Texas and New Mexico: The University of Texas at El Paso, Master's thesis, 66 p.

Wen, C. L., 1983, A study of bolson fill thickness in the southern Rio Grande rift, southern New Mexico, West Texas, and northern Chihuahua: The University of Texas at El Paso, Master's thesis, 74 p.
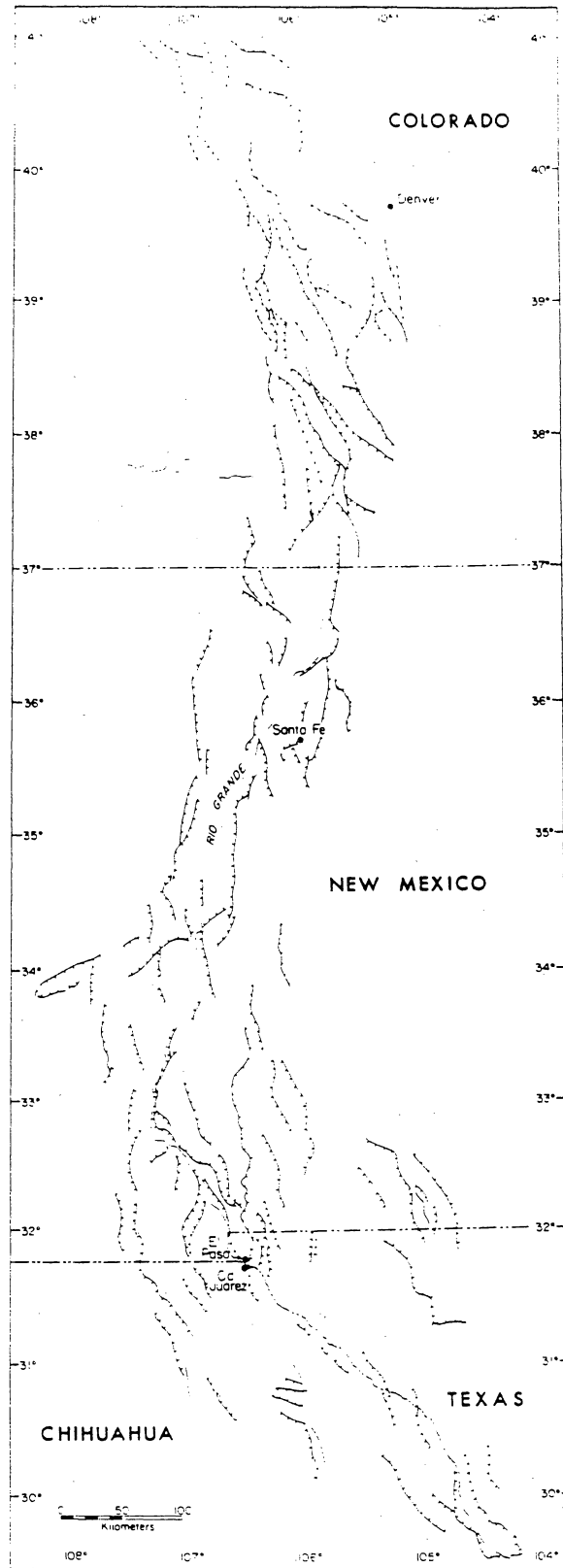
Figure 1. Index map of the Rio Grande rift showing generalized pattern of faulting (from Keller et al., 1990).
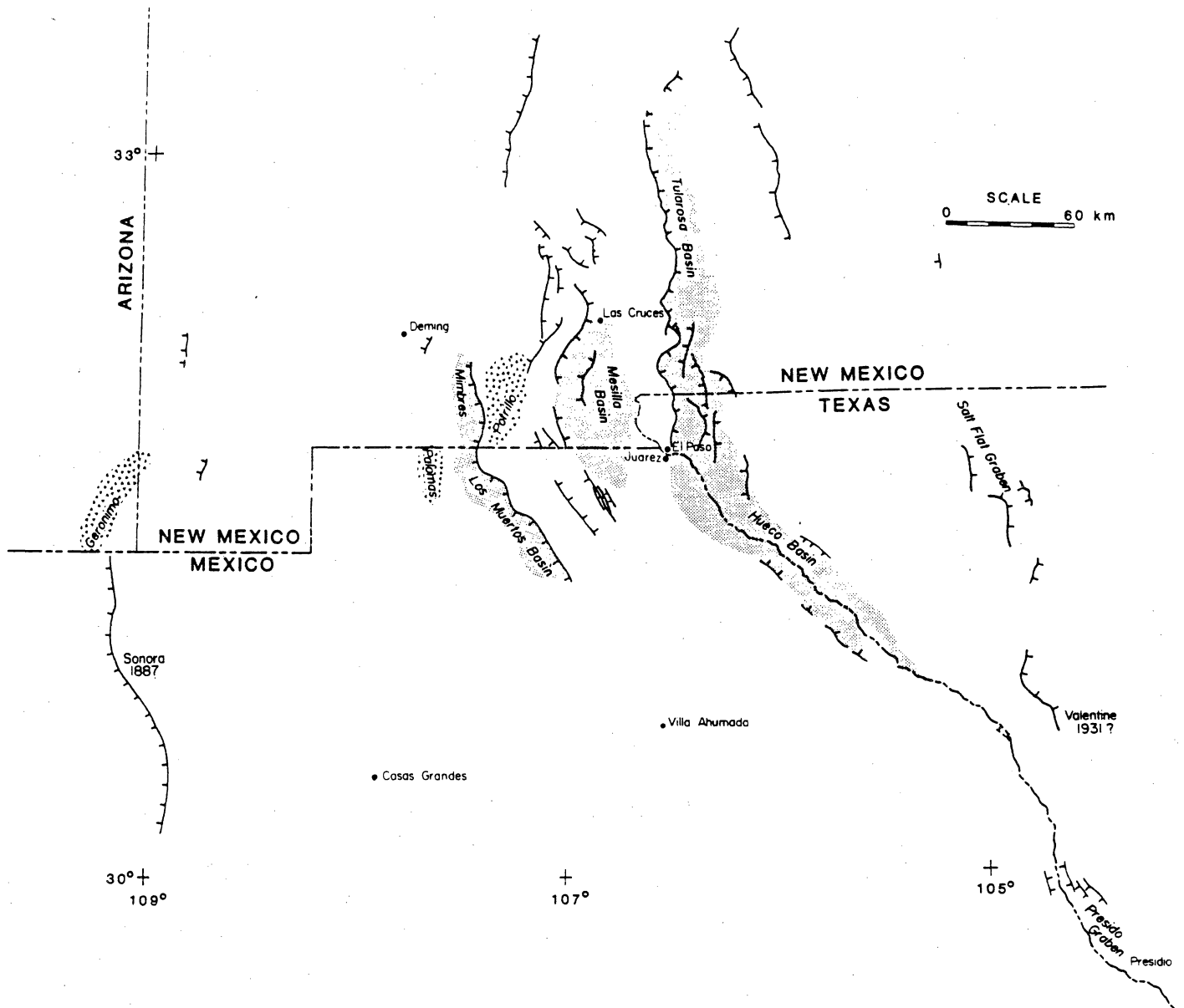
Figure 2. Index map of the southern Rio Grande rift showing generalized pattern of faults with Quaternary displacement. Stippled areas are Quaternary volcanic fields. Dates indicate faults that moved during the 1887 Sonora and 1931 Valentine earthquakes.
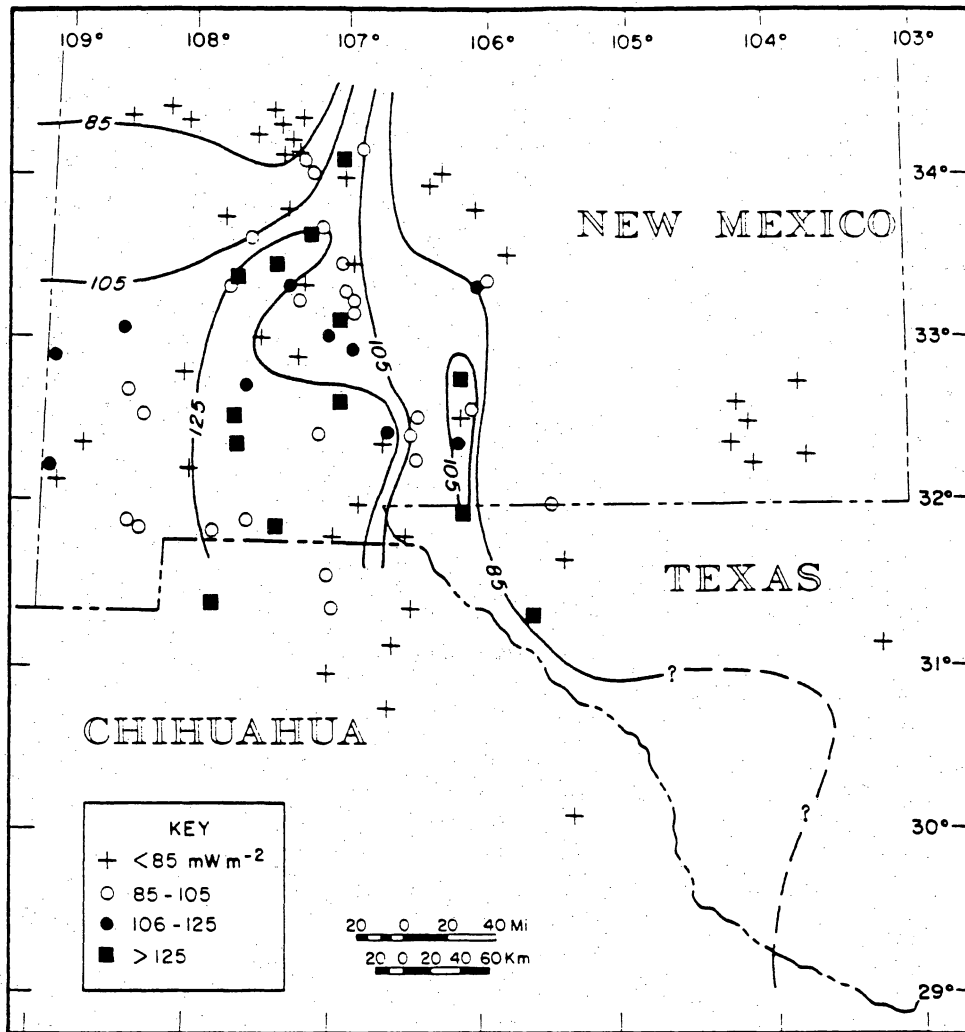
Figure 3. Heat flow data in the southern Rio Grande rift. Symbols indicate conventional heat flow measurements and values estimated from bottom-hole-temperature data. Contours are based on silica heat flow estimates (from Keller et al., 1990).
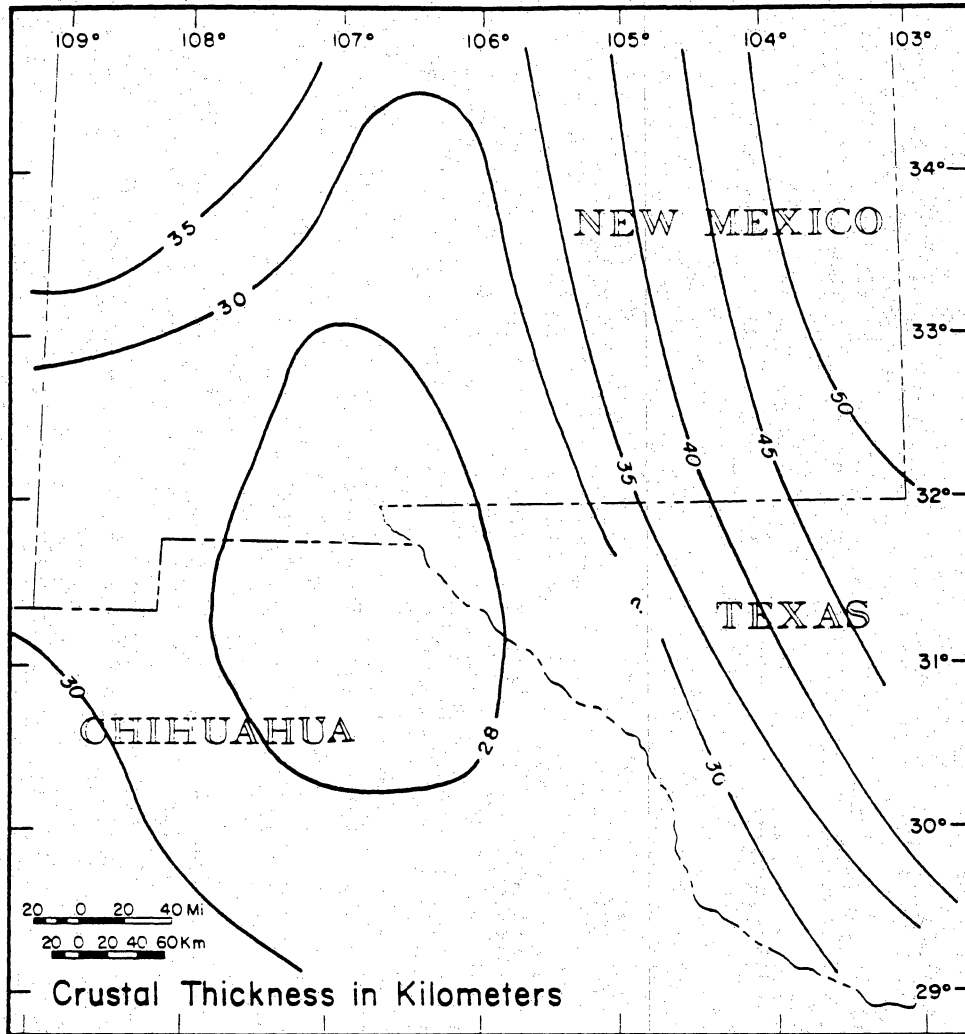
Figure 4. Contour map of crustal thickness in the southern Rio Grande rift. Contours are of depth to the Moho with sea level as a datum (from Keller et al., 1990).
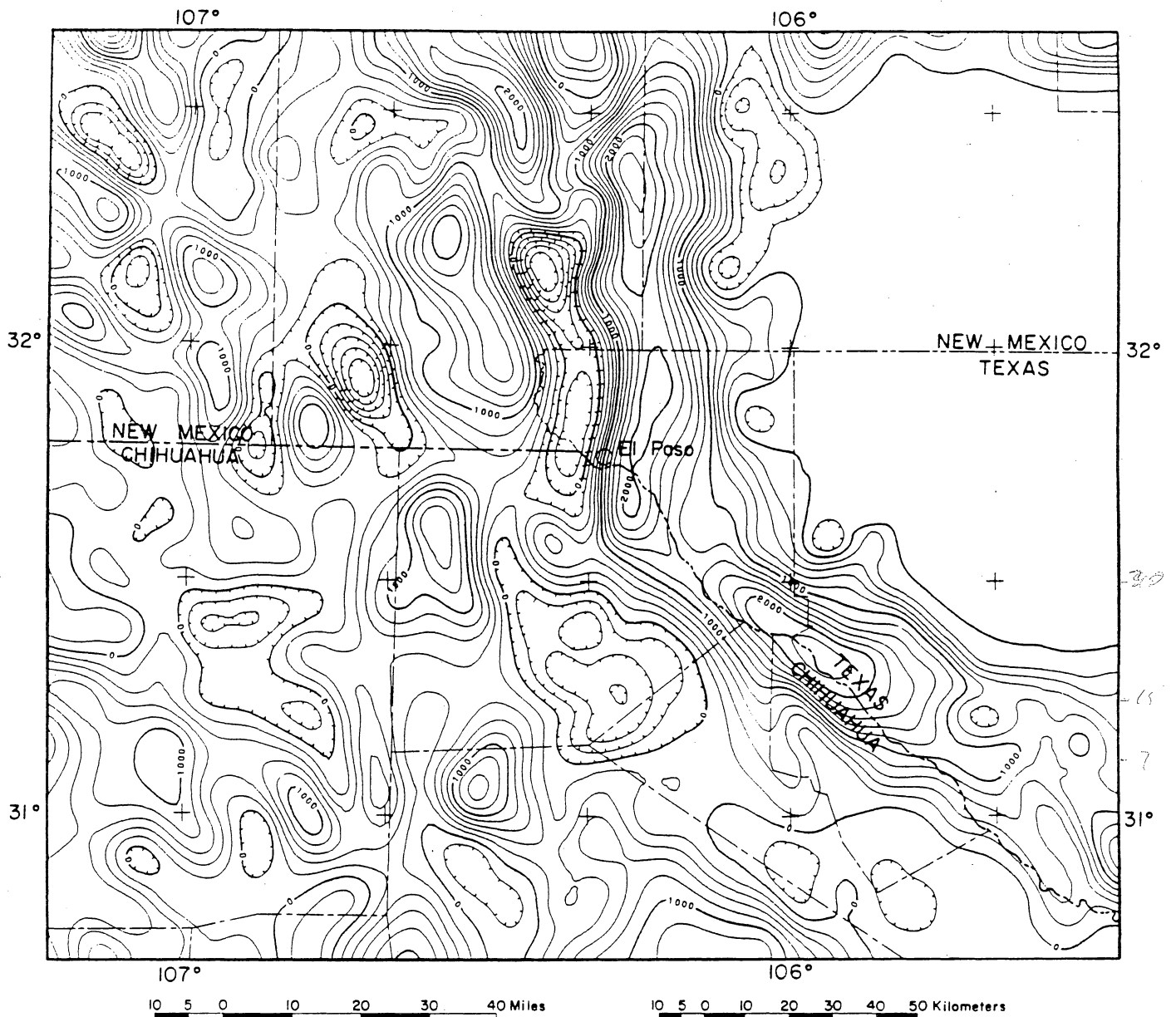
Figure 5. Contour map of the total estimated bolson fill thickness in the southern Rio Grande rift. These estimates where derived from a combined analysis of gravity and drilling data. Contour interval is 200 m (from Wen, 1983).
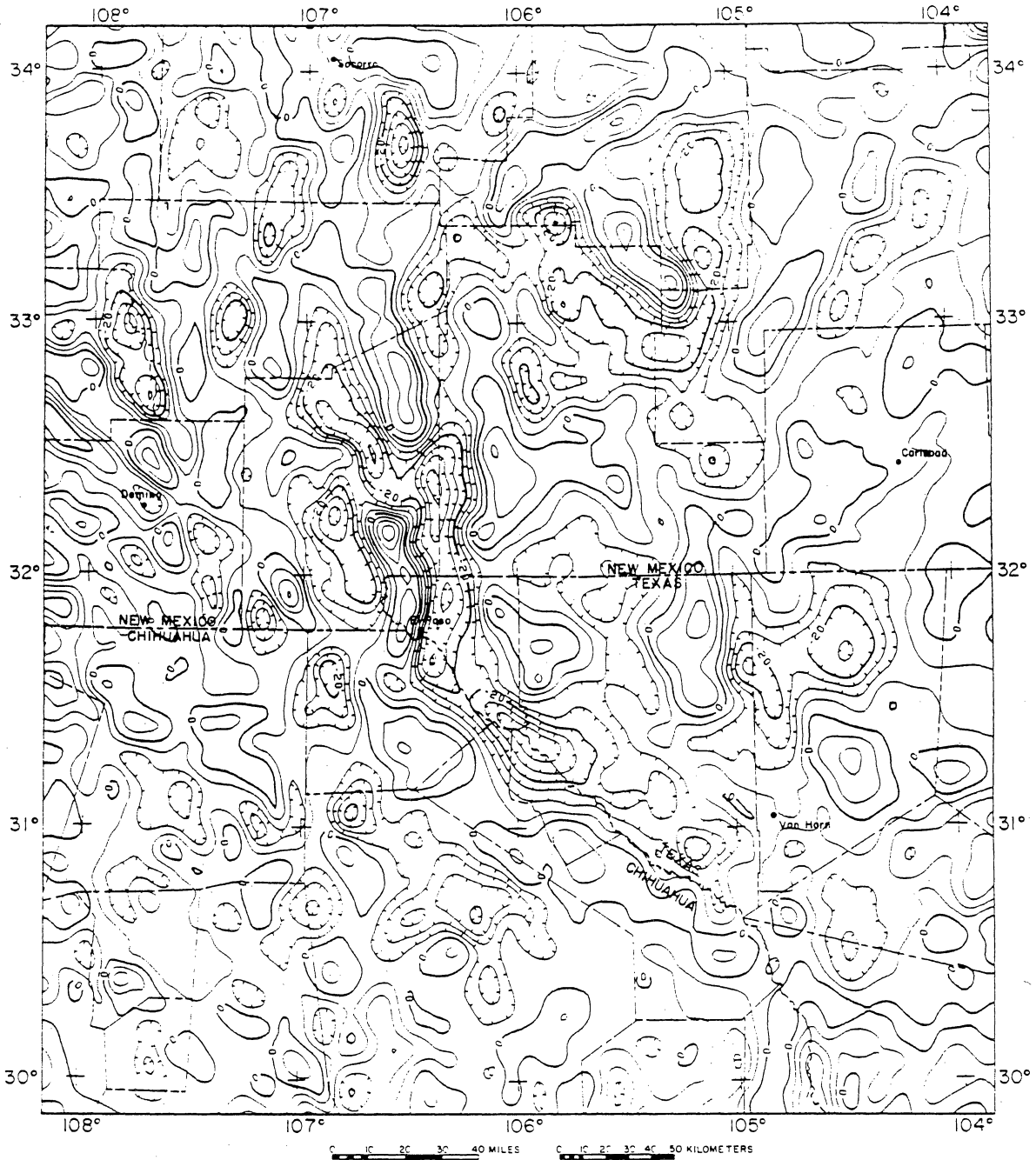
Figure 6. Residual gravity anomaly map of the southern Rio Grande rift. Contour interval is 5 mGal (from Dagget et al., 1986).

60
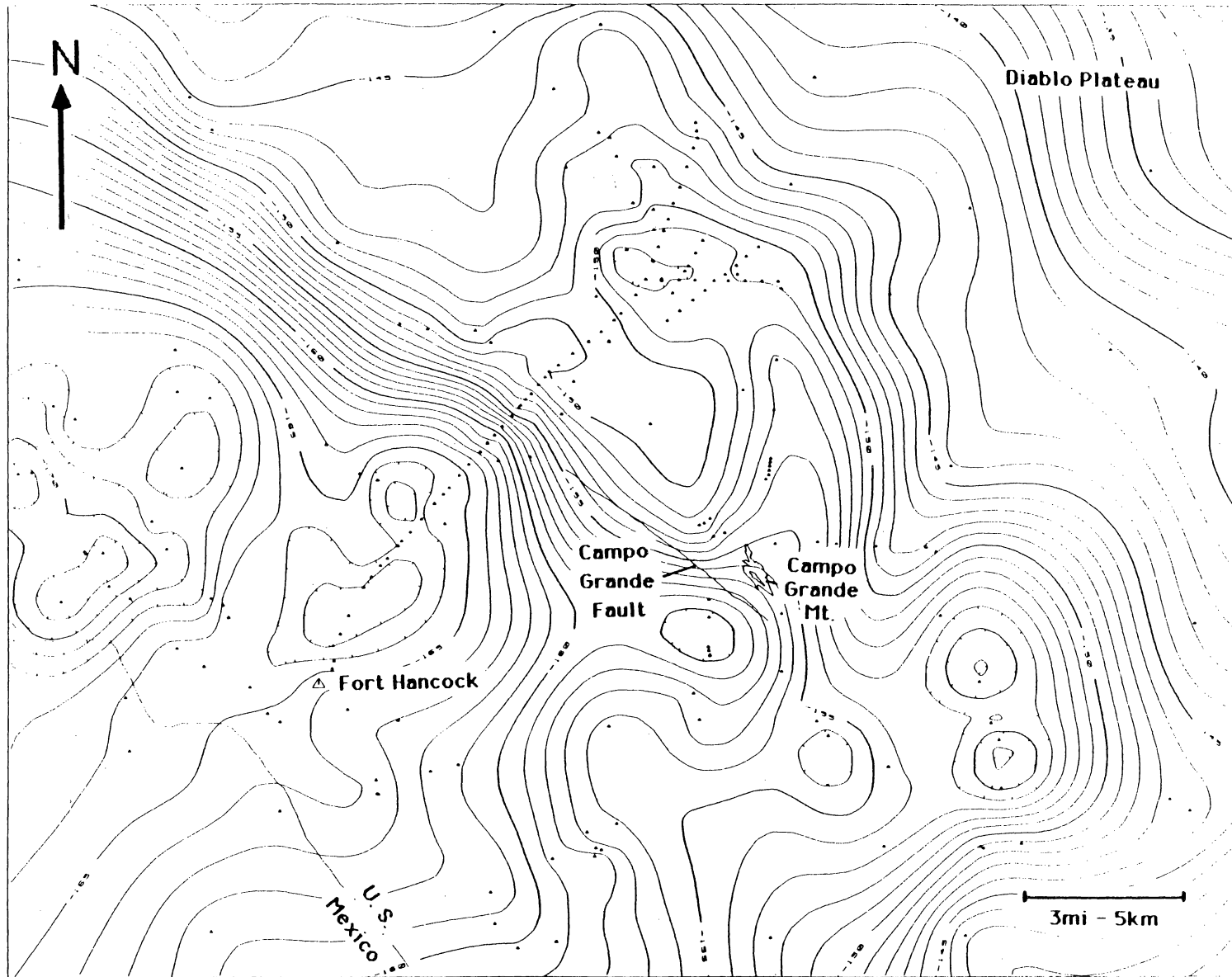
Figure 7. Bouguer gravity anomaly map of the Fort Hancock study area. Contour interval is 1 mGal.; sea level datum; reduction density - 2. 4 gm/cc.
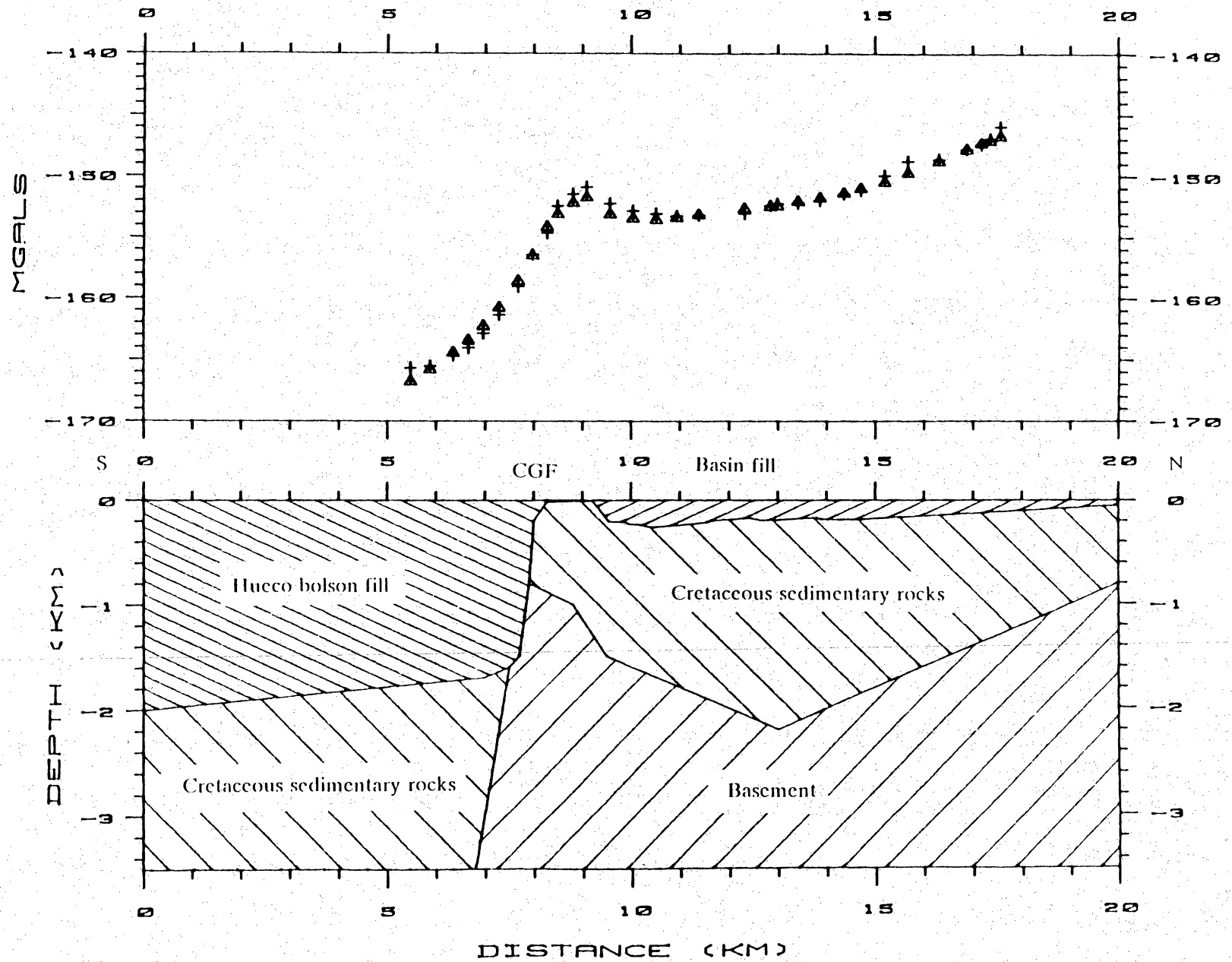
Figure 8. Gravity model representing generalized structural section across the proposed repository site area. CGF - Campo Grande fault. See text for description of the units shown and their densities.

ACKNOWLEDGMENTS